A CONTRACTION ARGUMENT FOR TWO-DIMENSIONAL SPIKING NEURON MODELS

ERIC FOXALL, RODERICK EDWARDS, SLIM IBRAHIM, P. VAN DEN DRIESSCHE

Abstract. A number of two-dimensional spiking neuron models that combine continuous dynamics with an instantaneous reset have been introduced in the literature. The models are capable of reproducing a variety of experimentally observed spiking patterns, and also have the advantage of being mathematically tractable. Here an analysis of the transverse stability of orbits in the phase plane leads to sufficient conditions on the model parameters for regular spiking to occur. The application of this method is illustrated by three examples, taken from existing models in the neuroscience literature. In the first two examples the model has no equilibrium states, and regular spiking follows directly. In the third example there are equilibrium points, and some additional quantitative arguments are given to prove that regular spiking occurs.

Key words. spiking neuron model, hybrid dynamical system, spike pattern, phase plane analysis, contraction mapping

AMS subject classification. 37N25

1. Introduction.

Formulating a model of individual neurons that is both biologically realistic and mathematically tractable is an important problem in mathematical neuroscience. The first significant model based on quantitative experiments is the classical Hodgkin-Huxley (H-H) model [7], which describes the dynamics of ionic channels in the cell membrane. It is an accurate model, however being a four-dimensional model it is difficult to analyze in detail. Various reductions of the H-H model have been achieved, of which the Fitzhugh-Nagumo (F-N) model [4] is an example. The F-N model is a two-dimensional continuous model, which is more easily analyzed than higher-dimensional systems. However, the autonomous F-N model cannot produce observed complex behaviours such as bursting and aperiodic spiking, since in two dimensions solutions tend either to an equilibrium state or to a simple periodic orbit. In a short paper [8] published in 2003, Izhikevich introduced a two-dimensional hybrid model that combines continuous dynamics with an instantaneous reset, which is examined in greater detail in [9]. His model is the first example of a class of models outlined by Touboul and Brette in [16] that are at once capable of reproducing a variety of spiking patterns, and are amenable to analysis. They have also been fitted to experimental data. For example, the *adaptive exponential model* introduced in [1] has been successfully fitted to intracellular recordings of pyramidal cells [2].

Therefore, following [15] and [16], we consider models of the form:

$$\begin{aligned} v' &= F(v) - w + I \\ w' &= a(bv - w) \end{aligned} \tag{1.1}$$

Here v corresponds to the potential of a neuron, and w is called the adaptation variable. We assume that F is at least C^2, strictly convex, and $F'(v)$ goes to a negative limit as $v \to -\infty$ and to infinity as $v \to +\infty$. The quantity $I \in \mathbb{R}$ is a constant input current, and a and b are positive real parameters. Also, there is the following reset condition: given additional parameters $d > 0$, v_S and v_R, if $t_S \in \mathbb{R}$ is such that $v(t_S^-) = v_S$ then $v(t_S^+) = v_R$ and $w(t_S^+) = w(t_S^-) + d$, where $v(t_S^\pm) = \lim_{t \to t_S^\pm} v(t)$ and similarly for w. In other words, solutions $(v(t), w(t))$ satisfy the ordinary differential equations (ODEs) in (1.1), except when $v(t) \to v_S$, at which time the potential is instantaneously reset to the value v_R, and the adaptation variable w is incremented by the fixed amount d. In the phase plane, the vertical line $\{(v, w) : v = v_R\}$ is the *reset line*, and the vertical line $\{(v, w) : v = v_S\}$ is the *spiking line*. The event $v(t) \to v_S$ is called *spiking*, and the time t_S at which this occurs is the *spike time*. In general $v_S > v_R$ and v_S is fairly large, so that a spike corresponds to a large increase in the potential followed by a sudden drop. In what follows, models of this form are collectively referred to as "the model".

We are primarily interested in the spiking dynamics of the model, that is, the pattern of spikes produced by solutions of the model. Since the input I is assumed constant, the model is autonomous. Moreover, after each spike the potential is reset to the same value, and the adaptation variable is simply incremented by a constant. As observed in [16], the behaviour of a solution following a spike depends entirely on the value of the adaptation variable at spike time; we recall the following definition.

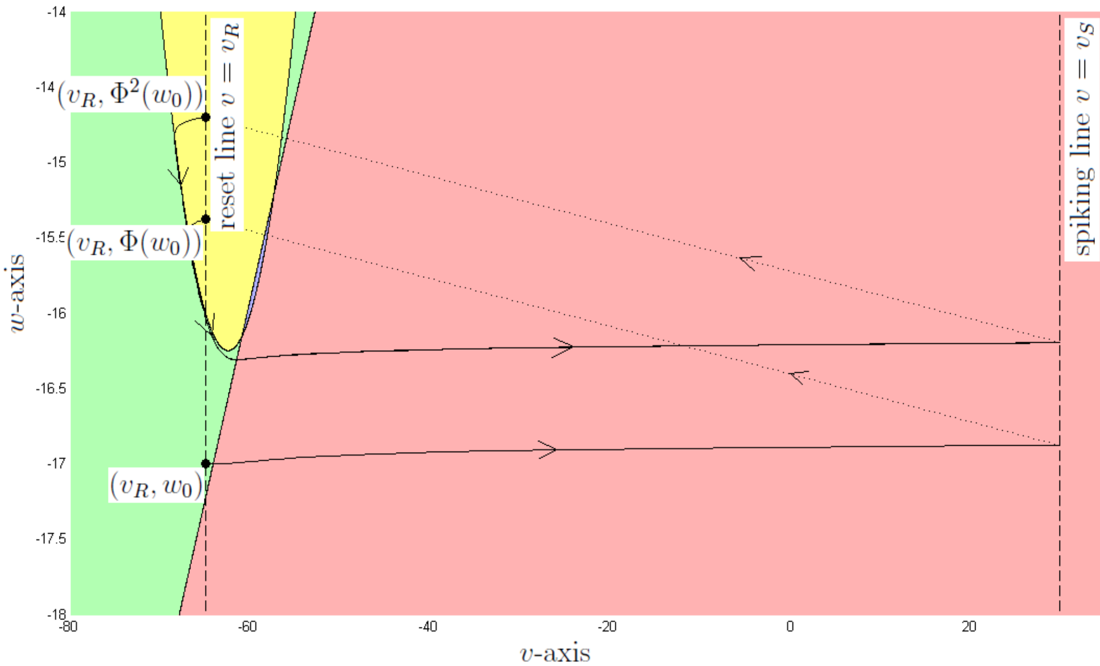

FIG. 1.1. *A solution of the model* (1.1)*. Trajectory begins at* (v_R, w_0) *and evolves towards the right, reaching the spiking line and resetting to* $(v_R, \Phi(w_0))$*. The trajectory continues from this point, making a half-turn before going towards the spiking line, and then resetting to* $(v_R, \Phi^2(w_0))$*.*

DEFINITION 1.1. *[16, Definition 2.3] Denote by* $\mathscr{D}$ *the set of adaptation values* w_0 *such that the solution of* (1.1) *with initial condition* (v_R, w_0) *reaches* v_S *in finite time. Let* $w_0 \in \mathscr{D}$*, and denote by* $(v(t), w(t))$ *the solution of* (1.1) *with initial condition* (v_R, w_0)*. Let* t_S *be the first time that* $v(t_S^-) = v_S$*. The* adaptation map Φ *is then the unique function such that*

$$\Phi(w_0) = w(t_S^-) + d$$

Intuitively, Φ maps the adaptation value following one spike to the adaptation value following the next spike, if another spike occurs (see Figure 1.1). Moreover, the orbit of the adaptation variable under the map Φ gives the spiking behaviour of a solution. For example, if after some number of iterations the adaptation value lands outside the domain of Φ, then the solution ceases to spike. If the adaptation value approaches a fixed point, then the solution ends up in a *regular* spiking pattern. If the adaptation value is attracted to a periodic orbit of period p, then the solution ends up in a periodic spiking or *bursting* pattern, with p spikes per burst. Aperiodic behaviour is also possible, in which spikes are emitted at irregular intervals and do not settle into a predictable pattern. These facts, and examples, are detailed in [16].

We are interested in conditions on the model parameters for global asymptotic stability of regular spiking, i.e., global asymptotic stability of a fixed point for Φ. We address the simplest case $\mathscr{D} = \mathbb{R}$, i.e., every initial condition on the reset line leads to the emission of infinitely many spikes. In [16] it is proved that Φ has a fixed point in this case and is at least continuously differentiable. Therefore, if Φ is *non-expansive*, i.e., $|\Phi'(w)| < 1$ for almost every $w \in \mathbb{R}$, then all orbits converge to a unique fixed point. This follows from the existence of a fixed point w_{fp} and from the fact that $|\Phi(w) - w_{fp}| \leq \int_{w_{fp}}^{w} |\Phi'(\zeta)| d\zeta$.

Now, the adaptation map is determined by the orbits, i.e., the paths traced out by trajectories in phase space. If orbits converge then Φ is non-expansive, and if orbits separate then it is possible that $|\Phi'| > 1$. A method described in [10] gives a sufficient condition for trajectories to converge towards one another over time. The variational equation (see (3.1)) can also be used to assess convergence of trajectories. However,

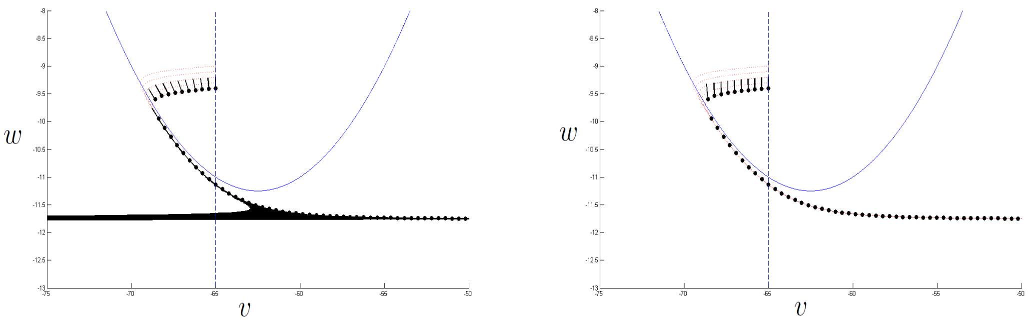

FIG. 1.2. *Evolution of displacement vectors along a trajectory. Displacement vectors portrayed as black lines. In (a), an initial displacement is placed in the vertical direction at the reset line, and then evolves according to the variational equation (3.1) for the model. In (b), the same applies, except that the component of the displacement which is tangent to the flow has been discarded, and only the component of the displacement which is perpendicular to the flow is displayed. Removal of the component which is tangent to the flow gives a set of vectors which is much better behaved (and appears almost to vanish entirely beyond some point along the trajectory).*

the orbits are invariant under reparametrization of the flow, therefore the convergence of orbits requires only the convergence of trajectories in any direction that is transverse to the flow. In other words, the stability of regular spiking depends only on the transverse convergence of trajectories. Our approach is to fix a transverse direction, onto which the variational equation is projected. The result is a quantity called the transverse local Lyapunov exponent (TLLE) which describes the rate of expansion of the transverse component of an initially transverse displacement. We express $\log|\Phi'|$ as the integral of the TLLE along trajectories, together with boundary terms that match the transverse direction to the reset and spiking lines. Using symmetry in the model equations, we estimate this integral and obtain sufficient conditions on the model parameters such that $\log|\Phi'| < 0$, i.e., such that Φ is non-expansive.

The TLLE is similar to the local Lyapunov exponent described in [3] and to the local divergence rate described in [5] and [13]; a comparison is made in Section 3. It is worth noting that the method described in Section 3 for obtaining the TLLE can be applied to any system determined by a twice continuously differentiable vector field and having a Poincaré map or a more general reset map of the type described here. For each choice of the transverse field an expression for the derivative of the map is obtained. A judicious choice of the transverse field may lead to a local exponent that has a convenient analytical or algebraic form, as is the case here, or that gives a more accurate measure of the separation of orbits than the variational equation, as shown in Figure 1.2.

In Section 2 we summarize enough from [16] to give the reader a sense of the phase plane for the model. In Section 3 we derive the TLLE and express Φ' as the integral of the TLLE over trajectories of the model. In Section 4 this integral is estimated, and when the model has ≤ 1 critical point, sufficient conditions are given on the parameters of the model for Φ to be non-expansive (see Theorem 4.4) i.e., for regular spiking to be globally asymptotically stable. In Section 5 we consider three examples. In the first two examples the result follows directly from Theorem 4.4. In the third example, the model has two critical points. For this example we adapt the results of Section 4 and measure the separation/convergence of orbits in the phase plane in order to show that regular spiking is globally asymptotically stable.

Note that the conditions given in Theorem 4.4 describe a relatively small region of parameter space. In [16] there are several results that describe the behaviour of Φ, including conditions for regular spiking, in terms of the values of Φ at certain points. The advantage of the present method is that it has a natural geometric interpretation in the phase plane, and conditions for regular spiking are given directly in terms of the model parameters.

2. Phase Plane. In this section we describe the phase plane for the model; a more detailed discussion can be found in [16]. As mentioned in the introduction, we assume that the domain $\mathscr{D}$ of the adaptation map is all of $\mathbb{R}$.

Both the cases $v_S = \infty$ and $v_S < \infty$ are considered. As shown in Proposition 2.1 in [16], if $v_S = \infty$ it is important to note that F must satisfy

$$\lim_{v\to\infty} F(v)/v^{2+\epsilon} \geq \alpha > 0 \tag{2.1}$$

for some $\epsilon > 0$ and some α in order to ensure that $w(t) < \infty$ as $t \to t_S^-$.

We now give some background on the phase plane for the model. Let $R = \{(v_R, w) : w \in \mathbb{R}\}$ denote the reset line. Let $X(v, w) = (f(v, w), g(v, w))^\top$ denote the vector field for the model, where $^\top$ denotes the transpose, and for $x_0 \in \mathbb{R}^2$ and t such that the flow is defined, let $\phi(t, x_0)$ denote the flow of X, i.e., $\phi(0, x_0) = x_0$ and $\phi'(t, x_0) \equiv \frac{d}{dt}\phi(t, x_0) = X(\phi(t, x_0))$. We are only interested in those solutions that start on the reset line, that is, $x_0 \in R$. By the assumption $\mathscr{D} = \mathbb{R}$, for each $x_0 \in R$ there is $w_S \in \mathbb{R}$ and $t_S > 0$ such that $\lim_{t\to t_S^-} \phi(t, x_0) = (v_S, w_S)$.

On the (v, w) plane $v' = 0$ whenever $w = F(v) + I$, and $w' = 0$ whenever $w = bv$; these equations give the v-nullcline and w-nullcline respectively. Let w^* and w^{**} be the intersection of R with the v-nullcline and w-nullcline respectively, i.e., $w^* = F(v_R) + I$ and $w^{**} = bv_R$. Then,

1. $w^* > w^{**}$,
2. for $w_0 < w^*$ and $x_0 = (v_R, w_0)$, $\phi(t, x_0)$ moves to the right towards the spiking line, and
3. for $w_0 > w^*$, $\phi(t, x_0)$ makes a half-turn counter-clockwise around (v_R, w^*) before intersecting R below w^*.

The proof of these facts is contained in [16]; a brief argument is given below. Note that a critical point is a point where the vector field vanishes.

Critical points satisfy $F(v) - bv + I = 0$. By the convexity of $F(v)$ and therefore of $F(v) - bv + I$, there are at most two critical points. If there are no critical points, by convexity of $F(v)$ the v-nullcline lies above the w-nullcline and $w^* > w^{**}$ (see Figure 2.1). Solutions with $w_0 < w^*$ are confined below the v-nullcline and move to the right, and solutions with $w_0 > w^*$ move initially to the left and down, intersect the v-nullcline moving straight down, and then move to the right, confined below the v-nullcline. When there is one critical point the nullclines intersect tangentially and the same is true. When there are two critical points denote them by $p_- = (v_-, w_-)$ and $p_+ = (v_+, w_+)$ with $v_- < v_+$. Note that the v-nullcline lies above the w-nullcline except when $v_- \leq v \leq v_+$ (see Figure 5.4 for an example). It follows from the convexity of F that $F'(v_-) < b$ and $F'(v_+) > b$. The Jacobian matrix

$$\begin{bmatrix} F'(v) & -1 \\ ab & -a \end{bmatrix}$$

has negative determinant at p_+, therefore p_+ is a saddle point. In Section 2.2 of [16] it is shown that the stable manifold Γ of the saddle point extends from p_+ down and towards the left at least to v_- below both nullclines; to see this, evolve the equations backwards in time. Since every initial condition on R leads to spiking, R and Γ are disjoint, therefore $v_R < v_-$, which implies that $w^* > w^{**}$ and that solutions with $w_0 > w^*$ make a half-turn. Since Γ is a continuous curve it is therefore confined to the half-plane $\{(v, w) : v > v_R\}$ and it must intersect the w-nullcline at some point (v, w) for which $v \leq v_-$, and this effectively prevents solutions with $w_0 < w^*$ from going above the w-nullcline, so that they have no choice but to move to the right towards the spiking line.

We can summarize the behaviour of solutions using the partition defined in Section 2.4 of [16]. If the model has ≤ 1 critical point let the *North*, *Center* and *South* regions be the sets that lie above, between, and below the nullclines respectively, as in Figure 2.1. If the model has two critical points, let the *North* region be the set $\{(w, v) : w \geq F(v) + I,\ w \geq bv\}$, the *Center* region be the set $\{(w, v) : F(v) + I < w < bv\}$ and the *South* region be the set $\{(w, v) : w \leq bv,\ w \leq F(v) + I\}$, and let the *West* and *East* regions be the

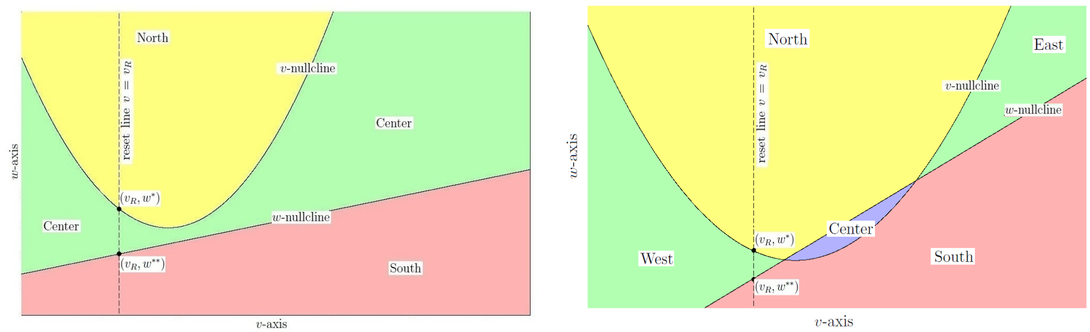

FIG. 2.1. *Phase plane for an example of model* (1.1) *with (a) no critical points and with (b) two critical points.*

left- and right-hand components respectively of the set $\{(w, v) : bv < w < F(v) + I\}$.

Then, if the model has ≤ 1 critical point, solutions that start on the reset line respect the order $North \to Center \to South$, i.e., no solution crosses from the South region into the North or Center regions, or from the Center region into the North region. If the model has two critical points, solutions that start on the reset line respect the order $North \to West \to South$. In the rest of this paper, we assume that solutions that start on the reset line intersect v_S in the South region; this holds trivially when $v_S = \infty$, and for most models used in practice this assumption holds.

3. Transverse Local Lyapunov Exponent. In this section we express $|\Phi'|$ as the integral of a transverse local Lyapunov exponent (TLLE) along trajectories. The end result, Theorem 3.7, is a sufficient condition for Φ to be non-expansive. For now, we assume that $v_S < \infty$, and generalize to $v_S = \infty$ in Section 3.6.

Note that from Section 3.3 onwards, where the more explicit computations begin, the unit vector field $\hat{X}$ replaces X. See the beginning of Section 3.3 for details. In particular, from Section 3.3 until the end of the paper, ϕ denotes the flow of $\hat{X}$, rather than X. Observe that each trajectory for X is a trajectory for $\hat{X}$.

If v_S is finite, then if t_S satisfies $\lim_{t \to t_S^-} \phi(t, w_0) = (v_S, \Phi(w_0) - d)$ as in Definition 1.1, $\phi(t_S, w_0)$ is well-defined and $\phi(t_S, w_0) = (v_S, \Phi(w_0) - d)$. The symbol $|\cdot|$ is used to denote both the absolute value in $\mathbb{R}$ and the Euclidean norm $\sqrt{v^2 + w^2}$ of a vector $(v, w) \in \mathbb{R}^2$.

3.1. Expression for Φ' using the variational equation. First of all, Φ' is expressed in terms of the general solution T to the variational equation, equation (3.1). Let $S = \{(t, x_0) \in \mathbb{R} \times \mathbb{R}^2 : \phi(t, x_0) \text{ is well-defined}\}$ and define the matrix-valued function $T : S \to M_2(\mathbb{R})$ by $T(0, x_0) = I_2$ where I_2 is the 2×2 identity matrix, and such that

$$\frac{d}{dt} T(t, x_0) = DX(\phi(t, x_0)) T(t, x_0) \tag{3.1}$$

Since X is continuously differentiable, $T(t, x_0)$ is the derivative of $\phi(t, x_0)$ with respect to x_0, that is,

$$\phi(t, x_0 + \epsilon u) - \phi(t, x_0) = \epsilon T(t, x_0) u + o(\epsilon) \tag{3.2}$$

for $u \in \mathbb{R}^2$ (for a proof, see for example Theorem 7.1 in [11]). Here $h(\epsilon) = o(\epsilon) \Leftrightarrow h(\epsilon)/\epsilon \to 0$ as $\epsilon \to 0$, where h denotes an arbitrary scalar- or vector-valued function. We would like to relate Φ' and T; Lemma 3.1 is the first step in this task. For $u, v \in \mathbb{R}^2$, $u^\top v$ is used to denote the dot product of u and v. Let $e_1 = (1, 0)^\top$ and $e_2 = (0, 1)^\top$ denote the standard basis vectors.

As mentioned in Section 1, it is assumed that all solutions with initial condition on the reset line $\{v = v_R\}$ reach the spiking line $\{v = v_S\}$ in finite time. As in Definition 1.1, for $w_0 \in \mathbb{R}$ and $x_0 = (v_R, w_0)$, let $t_S(w_0)$

denote the first time t such that $\phi(t, x_0)$ lies on the spiking line $\{v = v_S\}$. This gives a function

$$t_S : \mathbb{R} \to \mathbb{R}^+$$

The following property of t_S is proved.

LEMMA 3.1. *The function $t_S(w_0)$ is differentiable.*

Proof. Fix $w_0 \in \mathbb{R}$ and let $x_0 = (v_R, w_0)$. The implicit function theorem is used below to prove that t_S is differentiable at w_0.

Define $H(\tau, \epsilon) = e_1^\top(\phi(t_S(w_0) + \tau, x_0 + \epsilon e_2) - v_S$, and observe that $H(\tau, \epsilon) = 0$ if and only if $\phi(t_S(w_0) + \tau, x_0 + \epsilon e_2)$ lies on the spiking line $\{v = v_S\}$. It follows that $H(0, 0) = 0$ and $\partial_\tau H(0, 0) = e_1^\top X(\phi(t_S(w_0), x_0))$. The assumption that solutions spike in the South region (which lies below the v-nullcline) guarantees that $e_1^\top X(\phi(t_S(w_0), x_0)) \neq 0$. The implicit function theorem gives an open interval U containing 0 and a unique continuous function τ defined on U that is differentiable and satisfies $H(\tau(\epsilon), \epsilon) = 0$.

If $t_S(w_0 + \epsilon)$ is continuous for $\epsilon \in U$, then since $\phi(t_S(w_0 + \epsilon), x_0 + \epsilon e_2)$ lies on the spiking line, by the uniqueness of τ it follows that $t_S(w_0 + \epsilon) = t_S(w_0) + \tau(\epsilon)$ for $\epsilon \in U$, from which differentiability of t_S at w_0 follows. Therefore, suppose that $t_S(w_0 + \epsilon)$ fails to be continuous for some $\epsilon \in U$. Then there is a $\delta > 0$ and a sequence $(\epsilon_k) \to \epsilon$ such that $|t_S(w_0 + \epsilon_k) - t_S(w_0 + \epsilon)| \geq \delta$ for each $k \in \mathbb{N}$. There is a subsequence (ϵ_{k_n}) such that either

- $t_S(w_0 + \epsilon_{k_n}) \geq t_S(w_0 + \epsilon) + \delta$ for each n, or
- $t_S(w_0 + \epsilon_{k_n}) \leq t_S(w_0 + \epsilon) - \delta$ for each n.

In the first case, applying the result of the last paragraph with $t_S(w_0 + \epsilon)$ replacing $t_S(w_0)$, there is an open interval $\overline{U}$ containing 0 and a continuous function $\overline{\tau}$ defined on $\overline{U}$ that satisfies $\overline{\tau}(0) = 0$ and

$$t_S(w_0 + \epsilon_{k_n}) \leq t_S(w_0 + \epsilon) + \overline{\tau}(\epsilon_{k_n} - \epsilon) \tag{3.3}$$

since $\phi(t_S(w_0 + \epsilon) + \overline{\tau}(\epsilon_{k_n} - \epsilon), x_0 + \epsilon_{k_n} e_2)$ lies on the spiking line, but $t_S(w_0 + \epsilon_{k_n})$ is the *first* time t such that $\phi(t, w_0 + \epsilon_{k_n} e_2)$ lies on the spiking line. However, (3.3) is a contradiction since $\overline{\tau}(\epsilon_{k_n} - \epsilon) \to 0$ as $\epsilon_{k_n} \to \epsilon$. Therefore suppose $t_S(\epsilon_{k_n}) \leq t_S(w_0 + \epsilon) - \delta$ for each n. Since t_S is a positive function, the sequence $t_S(\epsilon_{k_n})$ is bounded, so it has a convergent subsequence with limit $t \leq t_S(w_0 + \epsilon) - \delta < t_S(w_0 + \epsilon)$. Since for each $n \in \mathbb{N}$, $\phi(t_S(\epsilon_{k_n}), x_0 + \epsilon_{k_n} e_2)$ lies on the spiking line, it follows by the continuity of ϕ that $\phi(t, x_0 + \epsilon e_2)$ lies on the spiking line, so that

$$t_S(w_0 + \epsilon) \leq t < t_S(w_0 + \epsilon)$$

which is a contradiction. It follows that $t_S(w_0 + \epsilon)$ is continuous for $\epsilon \in U$, and from the above discussion, this implies that $t_S(w_0)$ is differentiable at w_0. □

The following expression, given in (3.4), relates Φ' and T. Note that the assumption that solutions spike in the South zone guarantees that $(X^\perp(\phi(t_S, x_0)))^\top e_2 \neq 0$. The expression for Φ' given in (3.4) can be understood as "take a displacement in the e_2 direction at the reset line, evolve it along the trajectory, and then project onto the e_2 component of the (X, e_2) basis at the spiking line".

PROPOSITION 3.2. *Let T be defined as above, then for $x_0 = (v_R, w_0)$ and $w_0 \in \mathbb{R}$,*

$$\Phi'(w_0) = \frac{(X^\perp(\phi(t_S, x_0)))^\top}{(X^\perp(\phi(t_S, x_0)))^\top e_2} T(t_S, x_0) e_2 \tag{3.4}$$

Proof. From the definition of t_S it follows that $\phi(t_S(w_0), w_0) = (v_S, \Phi(w_0) - d)$; see Definition 1.1. Fix $x_0 = (v_R, w_0)$ and write $(\Phi(w_0 + \epsilon) - \Phi(w_0))e_2 = \phi(t_S(w_0 + \epsilon), x_0 + \epsilon e_2) - \phi(t_S(w_0), x_0)$ in two parts as

$$(\phi(t_S(w_0 + \epsilon), x_0 + \epsilon e_2) - \phi(t_S(w_0), x_0 + \epsilon e_2)) + (\phi(t_S(w_0), x_0 + \epsilon e_2) - \phi(t_S(w_0), x_0))$$

Let $\Delta t_S(w_0;\epsilon)$ denote $t_S(w_0+\epsilon)-t_S(w_0)$, then writing the Taylor expansion for ϕ with respect to the first argument, $\frac{d}{dt}\phi(t,x_0)=X(\phi(t,x_0))$ gives

$$\phi(t_S(w_0+\epsilon),x_0+\epsilon e_2)-\phi(t_S(w_0),x_0+\epsilon e_2))=\Delta t_S(w_0;\epsilon)X(\phi(t_S(w_0),x_0+\epsilon e_2))+o(\Delta t_S(w_0;\epsilon))$$

and (3.2) gives

$$\phi(t_S(w_0),x_0+\epsilon)-\phi(t_S(w_0),x_0)=\epsilon T(t_S,x_0)e_2+o(\epsilon)$$

By Lemma 3.1, t_S is differentiable, so that $\Delta t_S(w_0;\epsilon)=\epsilon t'_S(w_0)+o(\epsilon)=O(\epsilon)$ and

$$(\Phi(w_0+\epsilon)-\Phi(w_0))e_2=\epsilon t'_S(w_0)X(\phi(t_S(w_0),x_0+\epsilon e_2)+\epsilon T(t_S,x_0)e_2+o(\epsilon) \tag{3.5}$$

In order to remove the term involving t'_S, take the dot product with $(X^\perp(\phi(t_S,x_0+\epsilon e_2)))/(X^\perp(\phi(t_S,x_0+\epsilon e_2)))^\top e_2)$ on both sides. Then, divide by ϵ and take $\epsilon\to 0$ in (3.5) to obtain (3.4), which proves Proposition 3.2. ∎

3.2. Expression for Φ' in terms of the TLLE. Equation (3.4) is helpful in relating Φ' to the flow. However, it contains the term $T(t,x_0)$, which is the solution to a two-dimensional nonautonomous linear system, and in order to estimate Φ' it would be nice to replace the term $T(t,x_0)$ with something simpler. This is accomplished in the steps that follow by decomposing both the initial displacement e_2 and the evolution matrix $T(t,x_0)$ in terms of a basis that moves with the trajectory $\phi(t,x_0)$. To obtain such a basis, we define a transverse field, as follows.

Definition 3.3. *A vector field $Y:\mathbb{R}^2\to\mathbb{R}^2$ is* transverse *to a vector field $X:\mathbb{R}^2\to\mathbb{R}^2$ if $|(X(x))^\top Y(x)|<|X(x)||Y(x)|$ whenever $X(x)\neq 0$.*

If x is such that $X(x)\neq 0$, then it follows that $X(x)$ and $Y(x)$ are linearly independent, and so the projectors $P_X(x)$ and $P_Y(x)$ given by

$$P_X(x)=\frac{X(x)(Y^\perp(x))^\top}{(Y^\perp(x))^\top X(x)}\quad\text{and}\quad P_Y(x)=\frac{Y(x)(X^\perp(x))^\top}{(X^\perp(x))^\top Y(x)} \tag{3.6}$$

are well-defined and satisfy $I_2=P_X(x)+P_Y(x)$, where I_2 is the 2×2 identity matrix. This can be verified by writing $v\in\mathbb{R}^2$ as $v_1X(x)+v_2Y(x)$ and then applying the operators $P_X(x)$ and $P_Y(x)$.

The following function, called the transverse local Lyapunov exponent (TLLE) corresponding to the transverse field Y, appears in the result below:

$$L(x)\equiv\frac{(X^\perp(x))^\top[Y(x),X(x)]}{(X^\perp(x))^\top Y(x)} \tag{3.7}$$

Here $[Y,X]=DXY-DYX$ is the Jacobi bracket [6], also known as the commutator. The TLLE measures the rate of logarithmic expansion or contraction of a small transversal as it evolves along a trajectory. The TLLE is similar to the local Lyapunov exponent (l.l.e.) described in [3]. However, the l.l.e. measures the rate of expansion with respect to the asymptotic expanding direction, whereas in this case the TLLE measures the rate of expansion with respect to a chosen transverse direction. The TLLE can be more accurately described as a transverse version of the local divergence rate described in [5] and [13]. The present terminology is chosen because Lyapunov exponent is a more familiar term and the TLLE is indeed a local exponent for transverse displacements.

Proposition 3.4, given below, relates $\Phi'(w_0)$ to $L(x)$. The function $C(x)$, defined by

$$C(x)\equiv\frac{(X^\perp(x))^\top Y(x)}{(X^\perp(x))^\top e_2} \tag{3.8}$$

represents a boundary condition at the reset and spiking lines. It arises from the fact that Y and e_2 (the tangent vector to the reset and spiking lines) may not necessarily be parallel to one another. The integral in (3.9) can be understood as the net factor of expansion of a transversal, summed over a trajectory from the reset line to the spiking line.

Proposition 3.4. *Let $C(x)$ be defined as in (3.8) and let $L(x)$ be defined as in (3.7). Then for $w_0 \in \mathbb{R}$,*

$$\log|\Phi'(w_0)| = \int_0^{t_S} L(\phi(s,x_0))ds + \log\left|\frac{C(\phi(t_S,x_0))}{C(x_0)}\right| \tag{3.9}$$

Proof. Differentiating $X(\phi(t,x_0)$ with respect to t gives

$$\frac{d}{dt}X(\phi(t,x_0)) = DX(\phi(t,x_0))X(\phi(t,x_0)) \tag{3.10}$$

so that $X(\phi(t,x_0))$ solves the differential equation in (3.1). Replacing t with $t+\tau$ in (3.10) shows that $X(\phi(t+\tau,x_0))$ solves (3.1) as a function of t with initial condition $X(\phi(\tau,x_0))$. Multiplying both sides of the equation (3.1) on the right by $X(\phi(\tau,x_0))$ and using the fact that $T(0,x) = I_2$ for each x shows that $T(t,\phi(\tau,x_0))X(\phi(\tau,x_0))$ also solves (3.1) with initial condition $X(\phi(\tau,x_0))$. By uniqueness of solutions, this implies that

$$X(\phi(t+\tau,x_0)) = T(t,\phi(\tau,x_0))X(\phi(\tau,x_0)) \tag{3.11}$$

for t, τ and x_0 such that the above expression is defined. This may be interpreted as "T leaves X invariant". Using the projector $P_X(x)$ defined in (3.6) gives

$$T(t,x_0)P_X(x_0) = \frac{X(\phi(t,x_0))(Y^\perp(x_0))^\top}{(Y^\perp(x_0))^\top X(x_0)}$$

using (3.11) with $\tau = 0$. Write $T(t_S,x_0)$ as $T(t_S,x_0)I_2 = T(t_S,x_0)P_X(x_0) + T(t_S,x_0)P_Y(x_0)$. Plugging into (3.4), observe that $(X^\perp(\phi(t_S,x_0)))^\top$ annihilates $X(\phi(t_S,x_0))$ in $T(t_S,x_0)P_X(x_0)$, which leads to the expression

$$\Phi'(w_0) = \frac{(X^\perp(\phi(t_S,x_0)))^\top}{(X^\perp(\phi(t_S,x_0)))^\top e_2}T(t_S,x_0)Y(x_0)\frac{(X^\perp(x_0))^\top e_2}{(X^\perp(x_0))^\top Y(x_0)} \tag{3.12}$$

in which only the Y component of the initial displacement remains. Then, project $T(t_S,x_0)Y(x_0)$ onto the (X,Y) basis, letting

$$\mu(t,x_0) = \frac{(Y^\perp(\phi(t,x_0)))^\top T(t,x_0)Y(x_0)}{(Y^\perp(\phi(t,x_0)))^\top X(\phi(t,x_0))}$$

denote the X component and

$$m(t,x_0) = \frac{(X^\perp(\phi(t,x_0)))^\top T(t,x_0)Y(x_0)}{(X^\perp(\phi(t,x_0)))^\top Y(\phi(t,x_0))}$$

denote the Y component, so that $T(t,x_0)Y(x_0) = \mu(t,x_0)X(\phi(t,x_0)) + m(t,x_0)Y(\phi(t,x_0))$. Plugging this expression into (3.12), once again $(X^\perp(\phi(t_S,x_0)))^\top$ annihilates $X(\phi(t_S,x_0))$, which gives

$$\Phi'(w_0) = \frac{(X^\perp(\phi(t_S,x_0)))^\top Y(\phi(t_S,x_0))}{(X^\perp(\phi(t_S,x_0)))^\top e_2}m(t_S,x_0)\frac{(X^\perp(x_0))^\top e_2}{(X^\perp(x_0))^\top Y(x_0)} \tag{3.13}$$

This is a simpler expression than (3.4), since $m(t,x_0)$ satisfies the scalar differential equation (3.14) below. To derive this equation, note that $T(t,x_0)Y(x_0)$ solves the differential equation in (3.1), so that replacing $T(t,x_0)$ with $\mu(t,x_0)X(\phi(t,x_0)) + m(t,x_0)Y(\phi(t,x_0))$ in (3.1) gives

$$\frac{d\mu}{dt}X + \mu DXX + \frac{dm}{dt}Y + mDYX = (DX)(\mu X + mY)$$

Subtracting μDXX from both sides and taking the dot product with $X^\perp$ on both sides yields the equation

$$\frac{d}{dt}m(t,x_0) = L(\phi(t,x_0))m(t,x_0) \tag{3.14}$$

where $L(x)$, defined in (3.7), is the TLLE.

Observe that (3.14) is equivalent to the expression $\frac{d\log|m(t,x_0)|}{dt} = L(\phi(t,x_0))$, since any solution to (3.14) has constant sign. Taking the logarithm of the absolute value in (3.13), and using (3.14) and the fundamental theorem of calculus gives (3.9). □

Remark 1. *It follows from Proposition 3.4 that* Φ *is non-expansive whenever*

$$\int_0^{t_S} L(\phi(s,x_0))ds + \log\left|\frac{C(\phi(t_S,x_0))}{C(x_0)}\right| < 0 \tag{3.15}$$

We see that the above inequality is a condition for regular spiking that only requires estimating the integral of the function L along the flow ϕ, between the reset and spiking lines.

3.3. Choice of transverse fields. In the expression (3.15) the transverse field Y is still left unchosen. To estimate Φ', two choices of the transverse field are used. It is first useful to normalize the vector field X to unit vectors by defining

$$\hat{X}(x) \equiv X(x)/|X(x)|$$

when $X(x) \neq 0$ and $\hat{X}(x) \equiv 0$ when $X(x) = 0$. The trajectories of $\hat{X}$ are the same as those of X away from critical points, and a field of unit vectors has the convenient property that its solutions are parametrized by the arc length parameter. Since $\hat{X}$ is used in the computations in the rest of the paper, the notation ϕ is used to denote the flow for $\hat{X}$, rather than the flow for X as was previously the case. We write $\phi(r,x_0)$ rather than $\phi(t,x_0)$ to emphasize that the independent variable is now the arc length parameter and not time.

For the field of unit vectors $\hat{X}$, the TLLE with respect to a transverse field Y is obtained from (3.7) simply by replacing X with $\hat{X}$, which gives

$$L(x) \equiv \frac{(\hat{X}^\perp(x))^\top[Y(x),\hat{X}(x)]}{(\hat{X}^\perp(x))^\top Y(x)} \tag{3.16}$$

for the TLLE. Similarly, the boundary condition for the field $\hat{X}$ with respect to Y is given by

$$C(x) = \frac{(\hat{X}^\perp(x))^\top Y(x)}{(\hat{X}^\perp(x))^\top e_2} \tag{3.17}$$

The choice $Y = e_2 \equiv (0,1)^\top$ is called the *vertical* field, and the choice $Y = \hat{X}^\perp$ is called the *orthogonal* field. These fields are chosen because trajectories either go straight to the right towards the spiking line, in which $Y = e_2$ is convenient, or else trajectories make a half-turn before going towards the spiking line, in which case it is necessary to have Y turn with the trajectories, and $Y = \hat{X}^\perp$ is then the simplest choice. Note that

$$D\hat{X} = (I_2 - \hat{X}\hat{X}^\top)\frac{DX}{|X|}$$

when $X \neq 0$, where I_2 is the 2×2 identity matrix. This follows from the quotient rule, using the fact that $D|X| = D((X^\top X)^{1/2}) = X^\top DX/|X|$, and using $\hat{X} = X/|X|$ and $\hat{X}^\top = X^\top/|X|$.

If $Y = e_2$ then $DY = 0$. Recalling that $[Y,\hat{X}] = D\hat{X}Y - DY\hat{X}$ and substituting $Y = e_2$ in (3.16) gives

$$\begin{aligned} L_V &= \frac{(\hat{X}^\perp)^\top(I_2 - \hat{X}\hat{X}^\top)\left(\frac{DX}{|X|}e_2\right)}{(\hat{X}^\perp)^\top e_2} \\ &= \frac{(\hat{X}^\perp)^\top\left(\frac{DX}{|X|}e_2\right)}{(\hat{X}^\perp)^\top e_2} \end{aligned}$$

as the exponent for the vertical field. Using the representation $X = (f, g)^\top$ gives

$$DX = \begin{bmatrix} f_v & f_w \\ g_v & g_w \end{bmatrix} \tag{3.18}$$

where the subscripts denote partial derivatives with respect to v and w. Also, $\hat{X}^\perp = (-g, f)^\top/(f^2 + g^2)^{1/2}$. This gives

$$L_V = \frac{g_w f - f_w g}{f(f^2 + g^2)^{1/2}} \tag{3.19}$$

for the TLLE with respect to the vertical field. To find the boundary condition, set $Y = e_2$ in (3.17) and note that $(\hat{X}^\perp(\phi(t_S, x_0)))^\top e_2 \neq 0$ whenever x_0 lies on the reset line, as mentioned in the paragraph preceding Proposition 3.2. This gives

$$C_V = 1 \tag{3.20}$$

identically.

For the orthogonal field, substituting $Y = \hat{X}^\perp$ in (3.16) and using

$$D(\hat{X}^\perp) = (I_2 - \hat{X}^\perp(\hat{X}^\perp)^\top)\frac{D(X^\perp)}{|X|}$$

gives

$$\begin{aligned} L_O &= \frac{(\hat{X}^\perp)^\top(DX\hat{X}^\perp - D(\hat{X}^\perp)\hat{X})}{(\hat{X}^\perp)^\top\hat{X}^\perp} \\ &= (\hat{X}^\perp)^\top\left((I_2 - \hat{X}\hat{X}^\top)\frac{DX}{|X|}\hat{X}^\perp - (I_2 - \hat{X}^\perp(\hat{X}^\perp)^\top\frac{D(X^\perp)}{|X|}\hat{X})\right) \\ &= (\hat{X}^\perp)^\top\frac{DX}{|X|}\hat{X}^\perp \end{aligned}$$

after cancellation. Substituting for $\hat{X}^\perp$, for DX as in (3.18) and for $|X|$ and multiplying terms gives

$$L_O = \frac{g^2 f_v - fg(f_w + g_v) + f^2 g_w}{(f^2 + g^2)^{3/2}} \tag{3.21}$$

for the TLLE with respect to the orthogonal field. To find the boundary condition, set $Y = \hat{X}^\perp$ in (3.17) and use the same observation as for C_V in the denominator to find that

$$C_O(x) = \frac{1}{(\hat{X}^\perp(x))^\top e_2} \tag{3.22}$$

We distinguish the cases $w_0 < w^*$ and $w_0 > w^*$, using the results of Section 2. Recall that (v_R, w^*) is the unique point of intersection of the reset line with the v-nullcline.

3.4. Case $w_0 < w^*$. If $w_0 < w^*$ then for $x_0 = (v_R, w_0)$, $\phi(r, x_0)$ moves to the right, in which case the vertical field is a natural choice. Note that C_V, the boundary condition for the vertical field, is identically equal to 1, as given in (3.20). Let r_S be such that $\phi(r_S, x_0)$ is on the spiking line. From (3.9) this gives

$$\log|\Phi'(w_0)| = \int_0^{r_S} L_V(\phi(s, x_0))ds \tag{3.23}$$

and the sufficient condition

$$\int_0^{r_S} L_V(\phi(s, x_0))ds < 0 \tag{3.24}$$

for Φ to be non-expansive on $(-\infty, w^*)$.

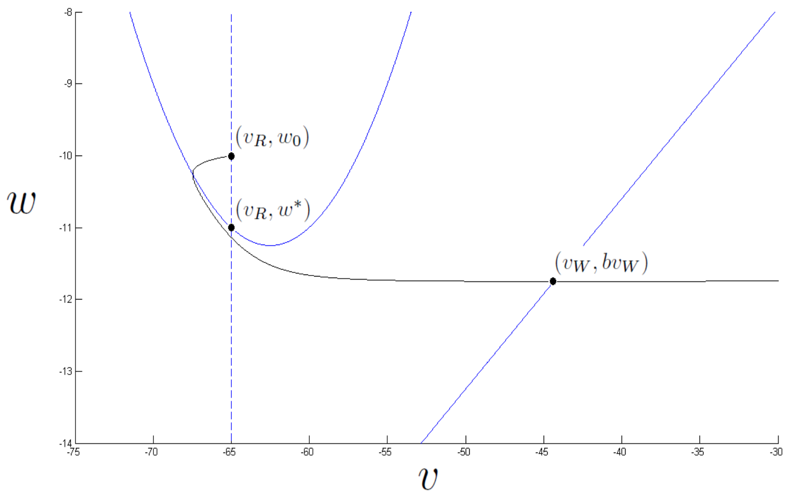

FIG. 3.1. *Depiction of a trajectory with* $w_0 > w^*$

3.5. Case $w_0 > w^*$. If $w_0 > w^*$ then for $x_0 = (v_R, w_0)$ it follows from the discussion in Section 2 that $\phi(r, x_0)$ has a unique point of intersection $p_W = (v_W, bv_W) = \phi(r_W, x_0)$ with the w-nullcline and moves to the right at least from p_W up to the spiking line, as shown in Figure 3.1. The orthogonal field is used from the reset line up to p_W and the vertical field is used from p_W up to the spiking line; since $w' = 0$ on the w-nullcline, $\hat{X}^\perp(p_W)$ and e_2 are parallel, i.e., the two fields line up at p_W. This gives

$$\log |\Phi'(w_0)| = \int_0^{r_W} L_O(\phi(s, x_0))ds + \int_{r_W}^{r_S} L_V(\phi(s, x_0))ds + \log \left| \frac{C_V(\phi(r_S, x_0))}{C_O(x_0)} \right| \tag{3.25}$$

From (3.20) and (3.22), $C_V = 1$ and $|C_O(x)| \geq 1$ for each x, so that $\log \left| \frac{C_V(\phi(r_S, x_0))}{C_O(x_0)} \right| \leq 0$. This gives the sufficient condition

$$\int_0^{r_W} L_O(\phi(s, x_0))ds + \int_{r_W}^{r_S} L_V(\phi(s, x_0))ds < 0 \tag{3.26}$$

for Φ to be non-expansive on (w^*, ∞). Abusing terminology somewhat, we refer to the integrals in (3.24) and to (3.26) as *contraction integrals*.

3.6. Extension to $v_S = \infty$. Here we show that the expressions in (3.23) and in (3.25) are valid when $v_S = \infty$. In [16] it is proved that if $F(v)/v^{2+\epsilon} \geq \alpha > 0$ for some α and some $\epsilon > 0$ as $v \to \infty$, and if a solution $(v(t), w(t))$ has $\lim_{t \to t_S^-} v(t) = \infty$, then $\lim_{t \to t_S^-} w(t)$ exists and is finite. Therefore, in the case $v_S = \infty$ the adaptation map is defined as $\Phi(w_0) = \lim_{t \to t_S^-} w(t) + d$. Writing $\Phi(w_0; v_S)$ to emphasize the dependence on v_S,

$$\Phi(w_0; \infty) = \lim_{v_S \to \infty} \Phi(w_0; v_S)$$

As shown in the following proposition, the limit $\lim_{v_S \to \infty} \log |\Phi'(w_0; v_S)|$ also exists, and convergence is uniform with respect to w_0.

PROPOSITION 3.5. *Let J be equal to either $\{w > w^*\}$ or $\{w < w^*\}$. Then $\log |\Phi'(w_0; v_S)|$ converges uniformly for $w_0 \in J$, as $v_S \to \infty$.*

Proof. We show that the expressions given in (3.23) and (3.25) converge uniformly for $w_0 \in \{w < w^*\}$ and for $w_0 \in \{w > w^*\}$. Note that since $C_V = 1$ identically, the last term appearing in (3.25) has the constant value $\log|1/C_O(x_0)|$. Therefore it is enough to address convergence of

$$\int_0^{r_S} L_V(\phi(s,x_0))ds \tag{3.27}$$

for x_0 in the South region as $r_S \to \infty$, since the only r_S-dependent terms in (3.23) and (3.23) are of this form. Using v as the integration variable we have $ds = (1+(g/f)^2)^{1/2}dv$. Using $(f(v,w), g(v,w)) = (F(v)-w+I, a(bv-w))$ as in (1.1), by (3.19) $L_V = (g-af)/f(f^2+g^2)^{1/2}) = (g/f-a)/(|f|(1+(g/f)^2)^{1/2})$ and

$$\int_0^{r_S} L_V(\phi(s,x_0))ds = \int_0^{v_S} \frac{g/f-a}{|f|}dv \tag{3.28}$$

where g and f are integrated along the trajectory, i.e., $g = g(\phi(r(v),x_0))$, $f = f(\phi(r(v),x_0))$ and $r = r(v)$ is a function of v. For $v > v_+$, $F(v)+I > bv$ since the v-nullcline lies above the w-nullcline, and so $af = a(F(v)-w+I) > a(bv-w) = g$. Since f and g are positive below the w-nullcline, $g/f > 0$, so that $0 < g/f < a$. Using the constraint on $F(v)$ given in (2.1) and using $w < bv$, $f/v^{2+\epsilon} \geq (F(v)-bv+I)/v^{2+\epsilon} \geq \alpha > 0$ for v large enough. Thus, for v_S large enough,

$$\left|\int_{v_S}^{\infty} \frac{g/f-a}{|f|}dv\right| = \int_{v_S}^{\infty} \frac{a-g/f}{|f|}dv < \int_{v_S}^{\infty} \frac{a}{\alpha v^{2+\epsilon}}dv = \frac{a}{\alpha(1+\epsilon)v_S^{1+\epsilon}}$$

and the last quantity vanishes as $v_S \to \infty$, independently of x_0. This implies the uniform convergence, for x_0 in the South region, of (3.27) as $r_S \to \infty$. ▯

The preceding observations combine to produce the following result.

Proposition 3.6. *The adaptation map $\Phi(w_0)$ (see Definition 1.1) is differentiable in the case $v_S = \infty$ and $\log|\Phi'(w_0)|$ is given by*

$$\lim_{r_S\to\infty} \int_0^{r_S} L_V(\phi(s,x_0))ds$$

when $w_0 < w^*$ and by

$$\int_0^{r_W} L_O(\phi(s,x_0))ds + \lim_{r_S\to\infty} \int_{r_W}^{r_S} L_V(\phi(s,x_0))ds + \log\left|\frac{1}{C_O(x_0)}\right|$$

when $w_0 > w^*$, where $x_0 = (v_R, w_0)$.

Proof. Let (v_n) be any sequence of values of v_S such that $v_n \to \infty$, and define the sequences (Φ_n) and (Φ'_n) by $\Phi_n = \Phi(w_0; v_n)$ and $\Phi'_n(w_0) = \Phi'(w_0; v_n)$. It follows from Theorem 7.17 in [14] that on a common interval of definition J, if the sequence (Φ_n) converges pointwise and the sequence (Φ'_n) converges uniformly on J, then $\lim_{n\to\infty}\Phi_n = \Phi$ is differentiable and $\Phi' = \lim_{n\to\infty}\Phi'_n$ on J. Pointwise convergence of (Φ_n) is proved in [16] and uniform convergence of $(\log\Phi'_n)$ is proved in Proposition 3.5, for J equal to either $\{w > w^*\}$ or $\{w < w^*\}$. Let $w_0 \in \mathbb{R}$, $w_0 \neq w^*$ be arbitrary and let K be a closed and bounded interval that contains w_0 and is contained in either $\{w > w^*\}$ or $\{w < w^*\}$. From the continuity of $\log|\cdot|$, the sequence (Φ'_n) converges uniformly on K. The statement of the proposition then follows at w_0, using the continuity of log, the fact that $r_S \to \infty$ as $v_S \to \infty$, and using the fact that $C_V(\phi(r_S,x_0)) = 1$ identically. Since $w_0 \neq w^*$ is arbitrary, the result follows. ▯

The results of Section 3 are summarized in the following theorem.

Theorem 3.7. *Let $\mathscr{D}$ denote the domain of Φ (see Definition 1.1). Then, if $\mathscr{D} = \mathbb{R}$, Φ is non-expansive on $\mathbb{R}$ when (3.24) is satisfied for all $w_0 < w^*$ and (3.26) is satisfied for all $w_0 > w^*$. If $v_S = \infty$ the integrals in (3.24) and (3.26) with upper endpoint r_S become improper integrals.*

The above theorem gives a sufficient but not a necessary condition for Φ to be non-expansive. As discussed in the introduction, if Φ is non-expansive and its domain is the whole real line then regular spiking is globally asymptotically stable.

4. Estimation of the integral. In this section we show that (3.24) is satisfied when the model has ≤ 1 critical point, and give sufficient conditions for (3.26), without assumptions on the critical points. In the case of ≤ 1 critical point, Theorem 4.4 gives sufficient conditions on the model parameters for Φ to be non-expansive.

Note that $L_V(x)$ is undefined on the v-nullcline. For a trajectory $\phi(r, x_0)$ defined for r in an interval U and disjoint from the v-nullcline, as in (3.28) we let v be the integration variable, so that the integral of L_V over the trajectory is

$$\int_U L_V(\phi(s, x_0))ds = \int_{v(U)} \frac{g/f - a}{|f|} dv$$

where $v(U)$ denotes the range of v-values of $\phi(r, x_0)$ for $r \in U$, $g = g(\phi(r(v), x_0))$ and $f = f(\phi(r(v), x_0))$ where $r = r(v)$ is a function of v. The argument to the integrand, when it is not given explicitly for efficiency of notation, is to be understood in this way. When the model has ≤ 1 critical point, off the v-nullcline $L_V(x) < 0$ almost everywhere. This is because in this case the w-nullcline lies below the v-nullcline except maybe at a single point, i.e., $bv < F(v) + I$ almost everywhere, so that $g = a(bv - w) < a(F(v) - w + I) = af$, or $g/f - a < 0$ almost everywhere (note $f \neq 0$ off the v-nullcline). Therefore the following is true.

PROPOSITION 4.1. *If the model has ≤ 1 critical point, then the condition in* (3.24) *is satisfied, and the second term in* (3.26) *is negative.*

Thus, if the model has ≤ 1 critical point, then for Φ to be non-expansive it is sufficent to have

$$\int_0^{r_W} L_O(\phi(s, x_0))ds < 0 \tag{4.1}$$

for $\phi(r, x_0)$ as described in Section 3.5. When the nullclines cross, i.e., when there are two critical points, L_V is positive on the strip $\{(v, w) : v_- < v < v_+\}$, which indicates separation of the orbits on that strip; this fact is addressed in the example in Section 5.3.

In the rest of this section we focus on the integral in (4.1). This is the integral of L_O over trajectories whose initial point lies on the reset line above w^* and whose terminal point lies on the w-nullcline. Except in the statement of Theorem 4.4, in the rest of this section nothing is assumed about the critical points.

To estimate the integral, trajectories are split into two pieces and the integrand is split into three pieces. Given $\phi(r, x_0)$, let $(v_V, F(v_V)) = \phi(r_V, x_0)$ be its unique point of intersection with the v-nullcline. Then for $0 \leq r \leq r_V$, $\phi(r, x_0)$ is contained in the subset

$$A = \{(v, w) : v \leq v_R, w \geq F(v) + I\}$$

of the North region. Let v_T be the unique value of v such that $F'(v) = 0$, and let $w_T = F(v_T)$. Let $v_{max} = \max\{v_R, v_T\}$, and define the subset $B = \{(v, w) : bv \leq w \leq l(v)\}$ of the Center/West region, where

$$l(v) = \{(v, w) : w = F(v) + I, v \leq v_{max}\} \cup \{(v, w) : w = F(v_{max}) + I, v \geq v_{max}\}$$

is the line that coincides with the v-nullcline to the left of v_{max} and extends horizontally to the right of v_{max}; see Figure 4.1. Then, for $r_V \leq r \leq r_W$, $\phi(r, x_0)$ is contained in B. We split L_O into three parts:

$$L_O = G + H + J \tag{4.2}$$

where

$$G = \frac{g^2 F'}{(f^2 + g^2)^{3/2}}, \quad H = \frac{(1 - ab)fg}{(f^2 + g^2)^{3/2}}, \quad J = \frac{-f^2 a}{(f^2 + g^2)^{3/2}} \tag{4.3}$$

after substituting values in (3.21) for the partial derivatives of f and g according to (1.1). Now, J is everywhere negative, but G is positive when $F' > 0$, i.e., when $v > v_T$, and if $ab < 1$, which is assumed later, then H is non-negative when f and g have the same sign. Therefore we estimate the integrals of H and G.

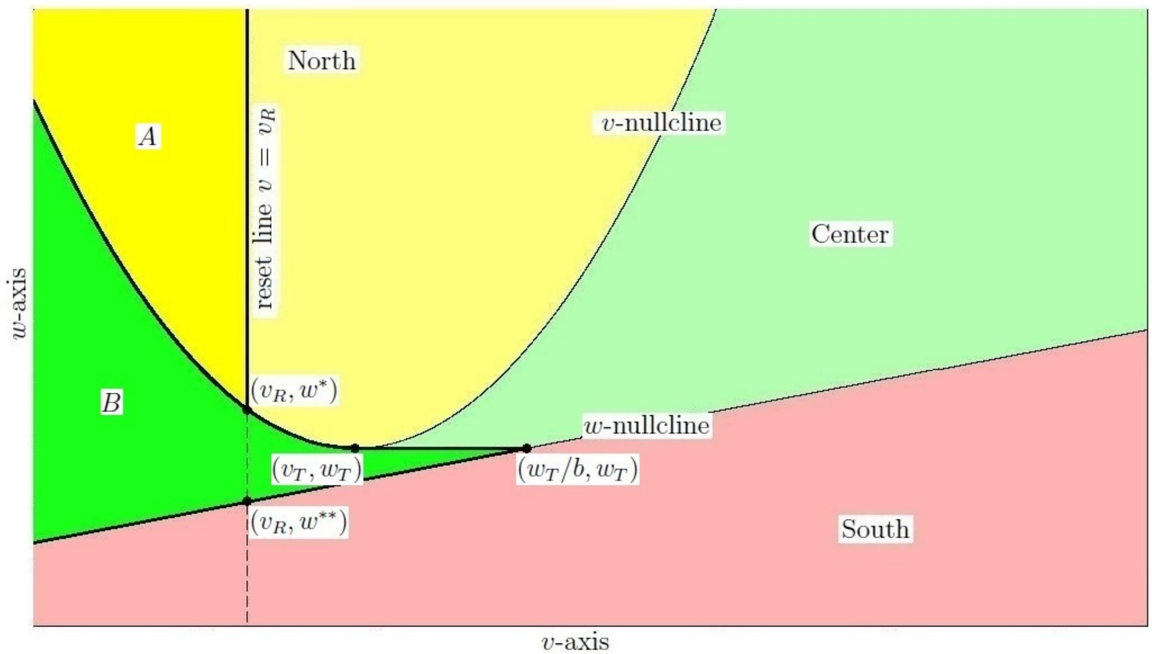

FIG. 4.1. *Phase plane for an example of model* (1.1), *with sets A and B bounded by the solid curves.*

4.1. Estimation of H. We give sufficient conditions for the integral of H along trajectories in the set $A \cup B$, i.e.,

$$\int_0^{\tau_W} \frac{(1-ab)fg}{(f^2+g^2)^{3/2}} ds \tag{4.4}$$

to be negative. The integral is taken along the first half of trajectories described in Section 3.5. Since s is the integration variable, trajectories are written $\phi(s, x_0)$.

PROPOSITION 4.2. *Suppose that $ab < 1$, $F'(v_R) < -a$ and $F'(v_R) + F'(w_T/b) < -2a$, where $w_T = F(v_T)$, and v_T is the unique value of v for which $F'(v) = 0$. Then the integral in* (4.4) *is negative.*

Proof. Let $z = f/g$, then z is well-defined on $A \cup B$ since $g \neq 0$ off the w-nullcline. First we show that $dz/ds \neq 0$, and then use z as the integration variable. Now

$$\frac{dz(\phi(s, x_0))}{ds} = (\nabla z)^\top \frac{d\phi(s, x_0)}{ds}$$

Since s is the arc length parameter, $d\phi(s, x_0)/ds = (f^2 + g^2)^{-1/2}(f, g)^\top$. Thus,

$$\begin{aligned}
\frac{dz}{ds} &= (f^2+g^2)^{-1/2}\big[f\partial_v z + g\partial_w z\big] \\
&= (f^2+g^2)^{-1/2}\big[f\frac{f_v g - f g_v}{g^2} + g\frac{f_w g - f g_w}{g^2}\big] \\
&= (f^2+g^2)^{-1/2}\big[-g_v(f/g)^2 + (f_v - g_w)(f/g) + f_w\big] \\
&= (f^2+g^2)^{-1/2}\big[-abz^2 + (F'+a)z - 1\big]
\end{aligned} \tag{4.5}$$

On A, $f \leq 0$ and $g < 0$ and so $z \geq 0$. Since $F'(v_R) < -a$ by assumption, $F'' > 0$ by convexity and $v < v_R$ on A it follows that $F' < -a$ on A. From this and from (4.5) it follows that $dz/ds < 0$ on A. In other words, trajectories starting on the reset line above w^* curve to the left between the reset line and the v-nullcline. Observe that $z < 0$ on B since $f > 0$ and $g < 0$ on B. If $dz/ds = 0$ at a point on B then

$$\frac{d}{ds}((f^2+g^2)^{1/2}\frac{dz}{ds}) = (-2abz + (F' + a))\frac{dz}{ds} + F''z = F''z < 0$$

since $F'' > 0$ and $z < 0$ on B. Also, $dz/ds = 0$ implies

$$\frac{d}{ds}((f^2+g^2)^{1/2}\frac{dz}{ds}) = (f^2+g^2)^{1/2}\frac{d^2z}{ds^2}$$

Therefore $dz/ds = 0 \Rightarrow d^2z/ds^2 < 0$ on B. In other words, if $\phi(s', x_0) \in B$ and $dz(\phi(s', x_0))/ds < 0$ then $dz(\phi(s, x_0))/ds < 0$ for all s such that $\phi(s'', x_0) \in B$ for $s' \leq s'' \leq s$. Now, $dz/ds < 0$ on the v-nullcline. Therefore, any trajectory that enters B by crossing the v-nullcline has $dz/ds < 0$ so long as it remains in B. This includes trajectories $\phi(s, x_0)$ with $x_0 = (v_R, w_0)$ and $w_0 > w^*$, for $r_V \leq s \leq r_W$. Thus, (4.4) can be re-written with z as the integration variable. Using (4.5) and the definition of z, (4.4) becomes

$$-\int_{z_2}^{z_1} \frac{1}{|g|}\frac{(1-ab)z}{(1+z^2)^{3/2}}\frac{ds}{dz}dz = \int_{z_2}^{z_1} \frac{(1-ab)z}{(1+z^2)}(abz^2 - (F'+a)z + 1)^{-1}dz \equiv \int_{z_2}^{z_1} Z(z)dz$$

In order for the above integral to be negative, it is sufficient that
1. $Z(z) < 0$ for $z_2 \leq z < 0$ and $Z(z) > 0$ for $0 < z \leq z_1$,
2. $[-z_1, z_1]$ lies in the domain of integration, and
3. $|Z(-z)| > |Z(z)|$ for $0 < z \leq z_1$.

Since $z = f/g \to -\infty$ as ϕ approaches the w-nullcline, Point 2 holds. Also, $ab < 1$ by assumption and $dz/ds < 0$ on $A \cup B$, thus Point 1 holds. It can be checked by comparison that $F'(v(z)) + F'(v(-z)) < -2a$, for $0 < z \leq z_1$, is sufficient for Point 3 to hold. Since $z > 0$ on A and $z < 0$ on B, and since $F'' > 0$, this last expression is true whenever $F'(v_R) + F'(w_T/b) < -2a$. This is because v_R and w_T/b are the largest v values on A and B respectively. ∎

4.2. Estimation of G. We estimate the integral of G along trajectories on $A \cup B$. Let $F'(v_R) < 0$, then G is negative on A, therefore we focus on the integral of G along trajectories on B, which is given by

$$\int_{r_V}^{r_W} \frac{g^2F'}{(f^2+g^2)^{3/2}}ds \tag{4.6}$$

Since s is the integration variable, trajectories are written $\phi(s, x_0)$. The integral is taken along trajectories with $x_0 = (v_R, w_0)$ where $w_0 > w^*$, $\phi(r_W, x_0) = (v_W, bv_W)$, as in Section 3.5, and $\phi(r_V, x_0) = (v_V, F(v_V))$ for some v_V, i.e., $\phi(r_V, x_0)$ lies on the v-nullcline.

PROPOSITION 4.3. *Suppose that $F'(v_R) < 0$. Let v_T denote the unique v such that $F'(v) = 0$, and let $w_T = F(v_T)$. Then the integral in (4.6) is negative when $F(v_R) \geq F(w_T/b)$.*

Proof. To estimate the integral in (4.6) we use the value of $F(v)$ on path segments as the integration variable. Note that the function $F(v)$ is two-to-one and with the exception of $F(v_T)$, each point in its range has one preimage to the left of v_T, and one preimage to the right of v_T. Let x_0 be fixed and ignore the point $\phi(r_V, x_0)$, then $\phi(s, x_0)$ lies below the v-nullcline and so it has $v' > 0$ and admits the parametrization $\phi(v)$. Letting $\phi_- = \operatorname{ran}\phi(v) \cap \{(v, w) : v < v_T\}$ and $\phi_+ = \operatorname{ran}\phi(v) \cap \{(v, w) : v > v_T\}$, then ϕ_- and ϕ_+ admit the parametrizations $\phi_-(y)$ and $\phi_+(y)$, where $y = F(v)$. Note that $ds/dy = (ds/dv)(dv/dy)$ and that

$$\frac{ds}{dv} = \frac{(f^2+g^2)^{1/2}}{f} = (1 + (g/f)^2)^{1/2} \tag{4.7}$$

blows up only on the v-nullcline and

$$\frac{dv}{dy} = \frac{1}{F'} \tag{4.8}$$

blows up only when $v = v_T$, and both functions are non-zero. We can then write the integral in (4.6), with improper integrals implied at $F(v_V)$ and $F(v_T)$), as

$$-\int_{F(v_T)}^{F(v_V)} \frac{g_-^2F_-'}{(f_-^2+g_-^2)^{3/2}}\frac{ds_-}{dy}dy + \int_{F(v_T)}^{F(v_W)} \frac{g_+^2F_+'}{(f_+^2+g_+^2)^{3/2}}\frac{ds_+}{dy}dy$$

where $f_\pm = f(\phi_\pm(y))$ and similarly for the other functions. Let $x = (g/f)^2$. Using (4.7) and (4.8), this simplifies to

$$-\int_{F(v_T)}^{F(v_V)} \frac{x_-}{|f_-|(1+x_-)} dy + \int_{F(v_T)}^{F(v_W)} \frac{x_+}{|f_+|(1+x_+)} dy = -\int_{F(v_T)}^{F(v_4)} V_-(y)dy + \int_{F(v_T)}^{F(v_W)} V_+(y)dy$$

where the last equalities define $V_-(y)$ and $V_+(y)$. In order to show this integral is negative it is sufficient to show that

1. $F(v_V) - F(v_T) \geq F(v_W) - F(v_T)$ and that
2. $V_-(y) > V_+(y)$ for $F(v_T) < y \leq F(v_W)$

Since $F(v_V) > F(v_R)$ and $F(w_T/b) > F(v_W)$ for all path segments, for Point 1 to hold it is sufficient that $F(v_R) \geq F(w_T/b)$. To verify Point 2, it is sufficient to have $f_-(y) < f_+(y)$ and $x_-(y) > x_+(y)$, since $d(x/(1+x))/dx > 0$. Note that if $\phi(v) = (v, w(v))$, then $dw(v)/dv = g/f < 0$ on B. Therefore, $w_-(y) > w_+(y)$, so that

$$f_-(y) = y - w_-(y) + I < y - w_+(y) + I = f_+(y)$$

Then, since $b > 0$ and $dw/dv < 0$,

$$dg(\phi(v))/dv = a(b - dw(v)/dv) > 0$$

and since g is negative, this gives

$$|g_-(y)| > |g_+(y)|$$

so that $x_-(y) > x_+(y)$, and the proposition is proved. □

REMARK 2. *Note that if F is symmetric about v_T, then the condition in Proposition 4.3 reduces to $v_R + w_T/b \leq 2v_T$. In particular, this is the case when $F(v) = v^2$.*

We summarize the main result of this section.

THEOREM 4.4. *Suppose the model* (1.1) *has ≤ 1 critical point. Let v_T be the unique v for which $F'(v) = 0$, and let $w_T = F(v_T)$. Suppose that $ab < 1$, $F'(v_R) < -a$, $F'(v_R) + F'(w_T/b) < -2a$ and $F(v_R) \geq F(w_T/b)$. Then all orbits under Φ converge to a unique fixed point.*

Proof. If there is at most one critical point then by Proposition 4.1, the condition in (3.24) is satisfied, which implies that $|\Phi'| < 1$ on $(-\infty, w^*)$. Together, Propositions 4.1, 4.2 and 4.3 imply (3.26), so that $|\Phi'| < 1$ on (w^*, ∞). Since $|\Phi'| < 1$ almost everywhere, Φ is non-expansive, and so its fixed point is unique and globally attracting. □

The conditions in Theorem 4.4 can be understood in the following way. If $a > 0$ is a small parameter, i.e., if the dynamics of the adaptation variable w are slow, the conditions are more easily satisfied. It is necessary to have $v_R < v_T$, since from the convexity of F, it follows that $F'(v) < 0$ if and only if $v < v_T$. The last two conditions require the w nullcline to lie close to the v nullcline, and the reset line to lie sufficiently far to the left of v_T. This is because w_T/b is the v-value of the intersection of the horizontal line extending from $(v_T, F(v_T))$ with the w-nullcline; in order to keep $F'(w_T/b)$ and $F(w_T/b)$ small, it is necessary that this point of intersection not be too far to the right of v_T.

Theorem 4.4 gives sufficient conditions on the model parameters for all initial conditions on the reset line to converge to a regular spiking behaviour, when the model has at most one critical point.

5. Examples. In this section we present three examples, one each of the quartic model $F(v) = v^4 + 2av$ [15], the exponential model $F(v) = e^v - v$ [1] and the Izhikevich model $F(v) = 0.04v^2 + 5v + 140$ [8], and in each case it is proved that regular spiking occurs. In the first two examples, parameter values are chosen so that Theorem 4.4 applies, from which regular spiking follows. In the third example the vector field has two critical points, and we need to account for expansion on the strip $\{(v, w) : v_- < v < v_+\}$.

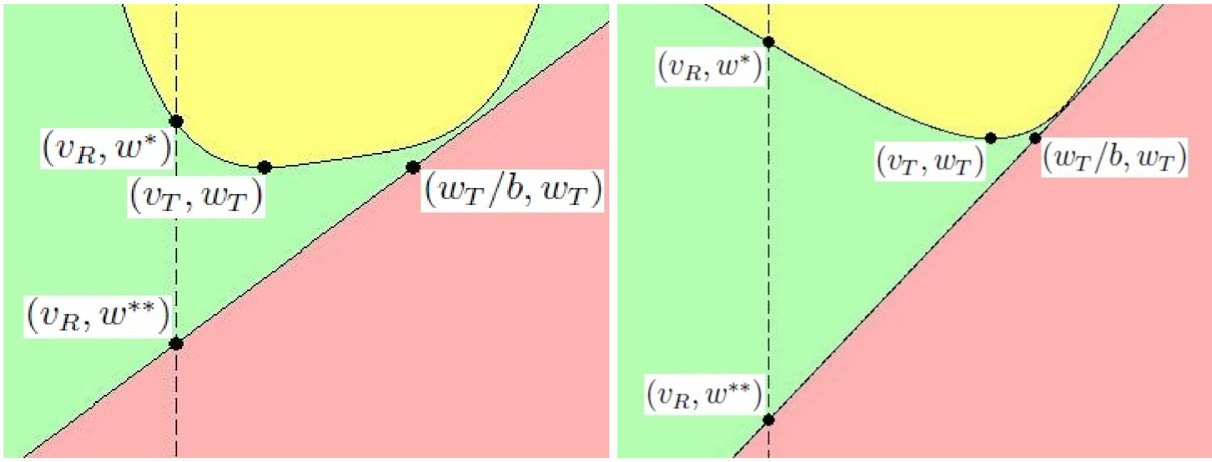

(a) Quartic model (b) Exponential model

FIG. 5.1. *Phase plane for the first two examples, neither of which have critical points*

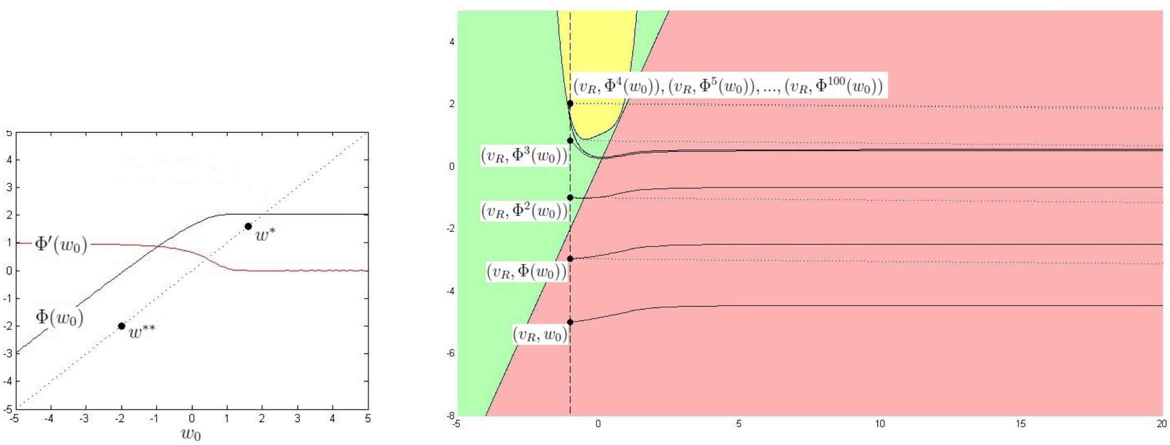

(a) Adaptation map (b) Numerical solution with initial condition $(-1, -5)$ and 100 spiking events; resetting portrayed by the dotted lines

FIG. 5.2. *Quartic model*

5.1. Quartic Model. Take the model (1.1) and let $F(v) = v^4 + 2av$, for the same a as in the equation for w' in the model (1.1). This is the quartic model described by Touboul in [15]. Taking the parameter values $a = 0.2, b = 2$, $I = 1$ and $v_R = -1$ gives the phase plane shown in Figure 5.1(a). Parameter values are chosen to illustrate the application of Theorem 4.4.

In this example the vector field has no critical points. Taking $d = 1.5$ and $v_S = \infty$ gives the adaptation map $\Phi(w_0)$ shown in Figure 5.2(a) (Φ is computed numerically). Observe that $|\Phi'(w_0)| < 1$ in the region shown, so that Φ is contracting in this region. Taking the initial condition $w_0 = -5$ on the reset line gives the solution shown in Figure 5.2(b), which appears to converge to a regular spiking pattern. To check that all initial conditions converge to regular spiking, it suffices to verify the conditions of Theorem 4.4. We readily compute that $ab = 0.4 < 1$, and that $F'(v_R) = 4(-1)^3 + 2(0.2) = -3.6 < -0.2 = -a$. Here v_T is given by $4v_T^3 + 2a = 0$ or $v_T = (-a/2)^{1/3} = (-0.1)^{1/3} \approx 0.46$, and $w_T = v_T^4 + 2av_T \approx 0.23$. $F'(w_T/b) \approx 0.41$ so that $F'(v_R) + F'(w_T/b) \approx -3.19 < -0.4 = -2a$, and $F(v_R) = (-1)^4 + 2a(-1) = 3.6$, $F(w_T/b) \approx 0.05$ so that $F(v_R) \geq F(w_T/b)$. Therefore, Theorem 4.4 applies and it follows that all initial conditions on the reset line lead to regular spiking.

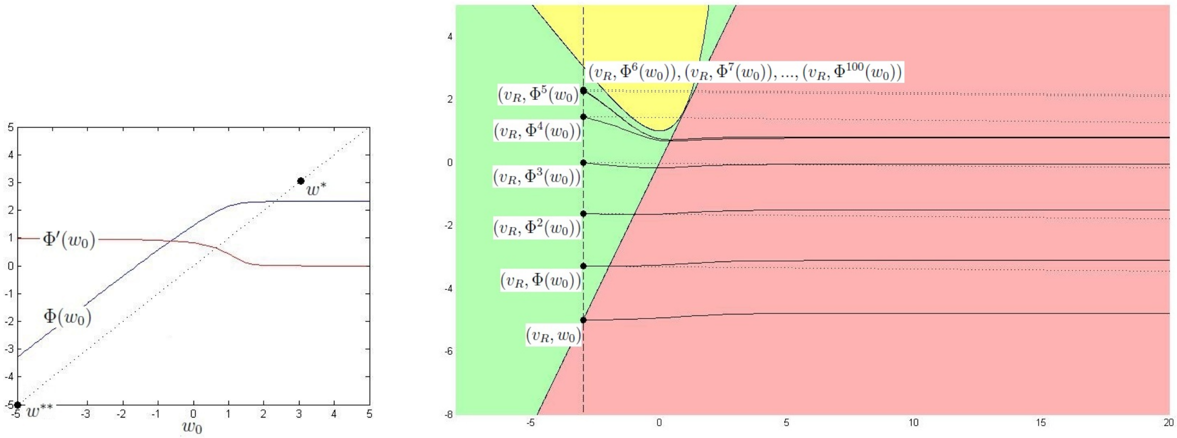

(a) Adaptation map

(b) Numerical solution with initial condition $(-3, -5)$ and 100 spiking events; resetting portrayed by the dotted lines

FIG. 5.3. *Exponential model*

5.2. Exponential model. Now, consider the model (1.1) with $F(v) = e^v - v$. This is the exponential model introduced by Brette and Gerstner in [1]. Taking parameter values $b = 5/3$, $I = 0$ and $v_R = -3$ gives the phase plane shown in Figure 5.1(b); parameter values are chosen to illustrate the application of Theorem 4.4. It can be checked that the vector field has no critical points.

Let $a = 0.05$. Taking $d = 1.5$ and $v_S = \infty$ gives the adaptation map shown in Figure 5.3(a). Observe that $|\Phi'(w_0)| < 1$ on the subset of its domain shown in the figure. Taking the initial condition $w_0 = -5$ on the reset line gives the solution shown in Figure 5.3(b) which appears to converge to a regular spiking pattern. To check that all initial conditions lead to regular spiking, it suffices to verify the conditions of Theorem 4.4. We compute $ab = 1/12 < 1$ and $F'(v_R) = e^{-3} - 1 \approx -0.95 < -0.05 = -a$. Then, v_T satisfies $F'(v_T) = 0$ or $e^{v_T} - 1 = 0$, so that $v_T = 0$, and $w_T = F(v_T) = 1$. $F'(w_T/b) = e^{3/5} - 1 \approx 0.82$, so that $F'(v_R) + F'(w_T/b) \approx -0.13 < -0.1 = -2a$ and $F(v_R) = e^{-3} - (-3) \approx 3.05$, $F(w_T/b) = e^{3/5} - 3/5 \approx 1.22$ so that $F(v_R) \geq F(w_T/b)$ and the conditions of Theorem 4.4 are satisfied. It follows that all initial conditions on the reset line lead to regular spiking.

Note that for this model, the slope of $F(v)$ rises sharply to the right of v_T, and goes monotonically towards -1 to the left of v_T, therefore the condition $F'(v_R) + F'(w_T/b) < -2a$ is difficult to satisfy. This is why in this example the v-nullcline and w-nullcline are taken so close to one another.

5.3. Izhikevich Model. Take now the model (1.1) with $F(v) = 0.04v^2 + 5v + 140$. This is known as the Izhikevich model [8]. Take the parameter values $I = 0$, $a = 0.005$, $b = 0.265$, $v_R = -65$, $v_S = 30$, and $d = 1.5$, which are used in [12] in simulations of the effect of deep brain stimulation on a network of neurons. This gives the phase plane shown in Figure 5.4, where the vector field has two critical points, denoted v_- and v_+ where $v_- < v_+$. For this model the domain of the adaptation map is the whole real line, that is, all initial conditions on the reset line lead to a spiking event (this can be checked via the method described in [16], Section 2.2).

A table of numerical values for this example is given below. Note that $w_T = F(v_T)$ and that $F(v_T)$ is the unique minimum for F. The values given for v_- and v_+ are approximate.

v_R	-65
w^*	-16
w^{**}	-17.225
v_T	-62.5
w_T	-16.25
v_-	-60.97
v_+	-57.41

The adaptation map is shown in Figure 5.5(a), and a numerical solution of the model is depicted in

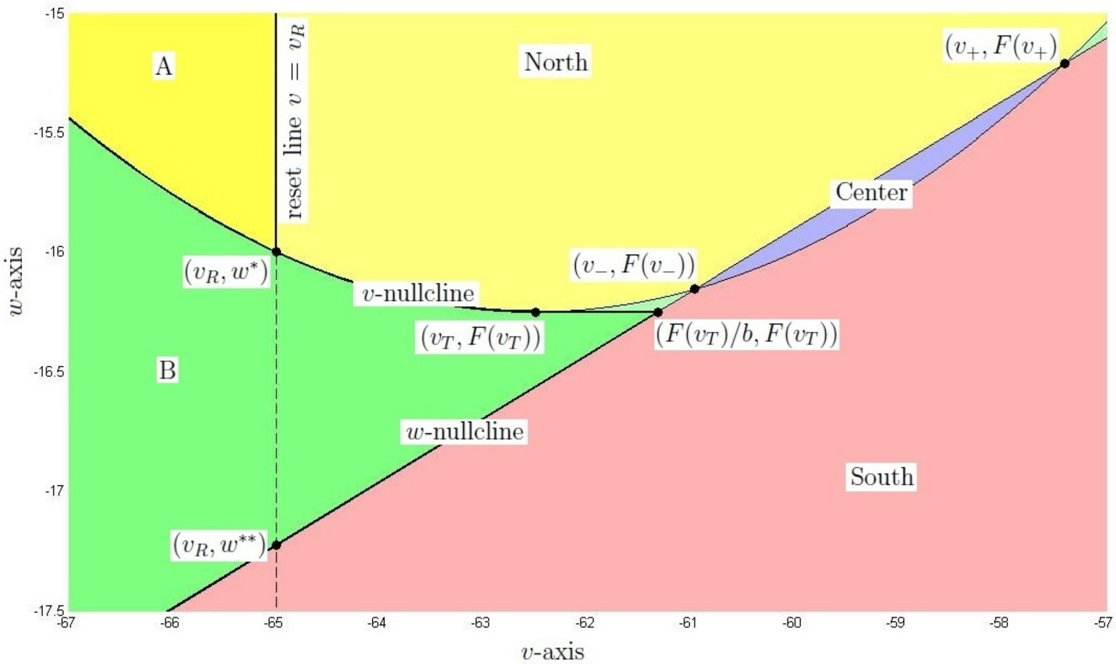

Fig. 5.4. *Phase plane for the Izhikevich model*

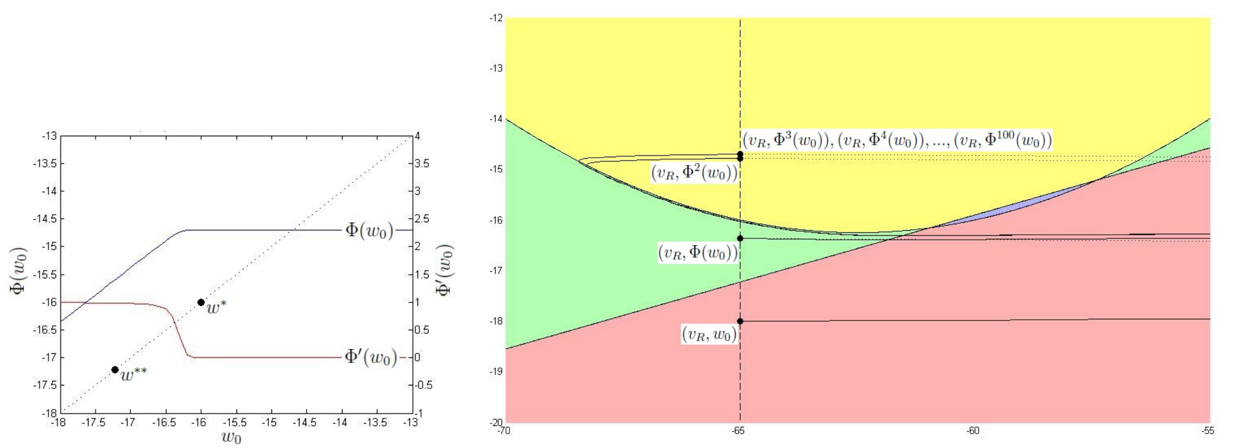

(a) Adaptation map

(b) Numerical solution with initial condition $(-65, -18)$ and 100 spiking events; resetting portrayed by the dotted lines

Fig. 5.5. *Izhikevich model*

Figure 5.5(b). Solution curves for one hundred spiking events are shown; after the third spike, subsequent solution curves are indistinguishable, therefore it appears that the solution is converging to a regular spiking behaviour. We want to prove that this is the case for all initial conditions, therefore our goal in this section is to prove the following theorem.

Theorem 5.1. *All initial conditions on the reset line lead to regular spiking.*

As discussed in the Introduction, to show that regular spiking occurs, we need to show that all orbits under Φ converge to a unique fixed point. The proof consists of two parts.

1. It is shown that all orbits under Φ eventually enter and remain in (w^*, ∞).
2. It is shown that the contraction integral (3.26) is negative for all path segments with initial point on the reset line above w^*, which implies that Φ is non-expansive on (w^*, ∞).

The result then follows from the discussion in the introduction. We begin the proof with Part 1.

PROPOSITION 5.2. *Given* $w_0 \in \mathbb{R}$, $\exists N \in \mathbb{N}$ *such that for* $n \geq N$, $\Phi^n(w_0) \in (w^*, \infty)$.

Proof. First we show that $\Phi((w^*, \infty)) \subset (w^*, \infty)$. It is enough to show for $w_0 > w^*$ that all paths beginning on (v_R, w_0) intersect the w-nullcline above $w^* - d$. Recall that w^{**} denotes the intersection of the reset line with the w-nullcline, that is, $w^{**} = bv_R$. Draw the line that has slope -0.1 and intersects the point (v_R, w^{**}). On this line, $\partial_v(g/f) = 0$ gives a quadratic equation in v. It can be checked by computation that this equation has two roots, one on either side of $v = -65$, and that $\partial_v(g/f) > 0$ when $v = -65$, which implies that the lesser root is a minimum of g/f. At this root, g/f is greater than -0.1, which implies that trajectories cross the line from the left. In particular, since $w^* = -16$ and $w^{**} = -17.225$, trajectories starting on the reset line above w^* must intersect the w-nullcline at a w value that is greater than $w^{**} > w^* - d$, and since $w' > 0$ below the w-nullcline, these trajectories are reset to a w-value that is greater than w^*.

Observe for $w_0 < w^{**}$ that $\Phi(w_0) \geq w_0 + d$ since w' is positive everywhere below the w-nullcline. Thus for any $w_0 \in \mathbb{R}$ there exists an N such that $\Phi^N(w_0) > w^{**}$. Since $\Phi(w^{**}) \geq w^{**} + d > w^*$ it follows that $\Phi^{N+1}(w_0) > w^*$. Then $\Phi(w^*, \infty) \subset (w^*, \infty)$ implies that $\Phi^n(w_0) > w^*$ for all $n \geq N + 1$. ∎

Part 1 is proved. In the next three propositions, we address Part 2. We are interested in trajectories $\phi(r, x_0)$ with $x_0 = (v_R, w_0)$ and $w_0 > w^*$. We want to show that

$$\int_0^{r_W} G(\phi(s, x_0)) + H(\phi(s, x_0)) + J(\phi(s, x_0))ds + \int_{r_W}^{r_S} L_V(\phi(s, x_0))ds < 0 \tag{5.1}$$

This is the contraction integral in (3.26) expressed with the notation from equation (4.2). In the following proposition we prove that the first two terms are negative.

PROPOSITION 5.3. *The terms* $\int_0^{r_W} G(\phi(s, x_0))ds$ *and* $\int_0^{r_W} H(\phi(s, x_0))ds$ *in the above integral are negative.*

Proof. Here $ab < 1$, $F'(v_R) = -0.2 < -a$ and $F'(v_R) + F'(w_T/b) \approx -0.11 < -2a$ so that the results of Proposition 4.2 hold. Also, $F(v)$ is symmetric, since it is quadratic, and $v_R + w_T/b \approx -126.32 < -125 = 2v_T$ and so the results of Proposition 4.3 hold (see the remark following Proposition 4.3). The result follows from these two propositions. ∎

Consider now the term $\int_{r_W}^{r_S} L_V(\phi(s, x_0))ds$. Since the model has two critical points, Proposition 4.1 does not apply. Indeed, L_V is positive if and only if

$$g = a(bv - w) > a(F(v) - w + I) = af$$

that is, when $bv > F(v) + I$, which is true on the strip $\{(v, w) : v_- < v < v_+\}$ and nowhere else. Using this fact, and using the identity given in (3.28) we find that

$$\int_{r_W}^{r_S} L_V(\phi(s, x_0))ds = \int_{v_W}^{v_S} \frac{g/f - a}{|f|} dv \leq \int_{v_-}^{v_+} \frac{g/f - a}{|f|} dv$$

where it is understood that $g = g(\phi(r(v), x_0))$, $f = f(\phi(r(v), x_0)))$ and $r = r(v)$ is a function of v. From this, from Proposition 5.3 and from equation (5.1), to show the contraction integral is negative it suffices to show that

$$\int_0^{r_W} J(\phi(s, x_0))ds + \int_{v_-}^{v_+} \frac{g/f - a}{|f|} dv < 0$$

As mentioned in Section 4.1, J is everywhere negative. We estimate both integrals, and show that the negative contribution outweighs the positive contribution. We begin with the positive contribution.

PROPOSITION 5.4.

$$\int_{v_-}^{v_+} \frac{g/f - a}{|f|} dv < 1.5 \times 10^{-3} \tag{5.2}$$

Proof. Since $f > 0$ in the South region, $\partial_w \frac{g/f - a}{|f|} = \partial_w \frac{g - af}{f^2} = \frac{2(g - af)}{f^3} > 0$ and $g - af > 0$ on (v_-, v_+). To bound the integral in (5.2) it suffices to evaluate it along a curve that lies above trajectories on the strip

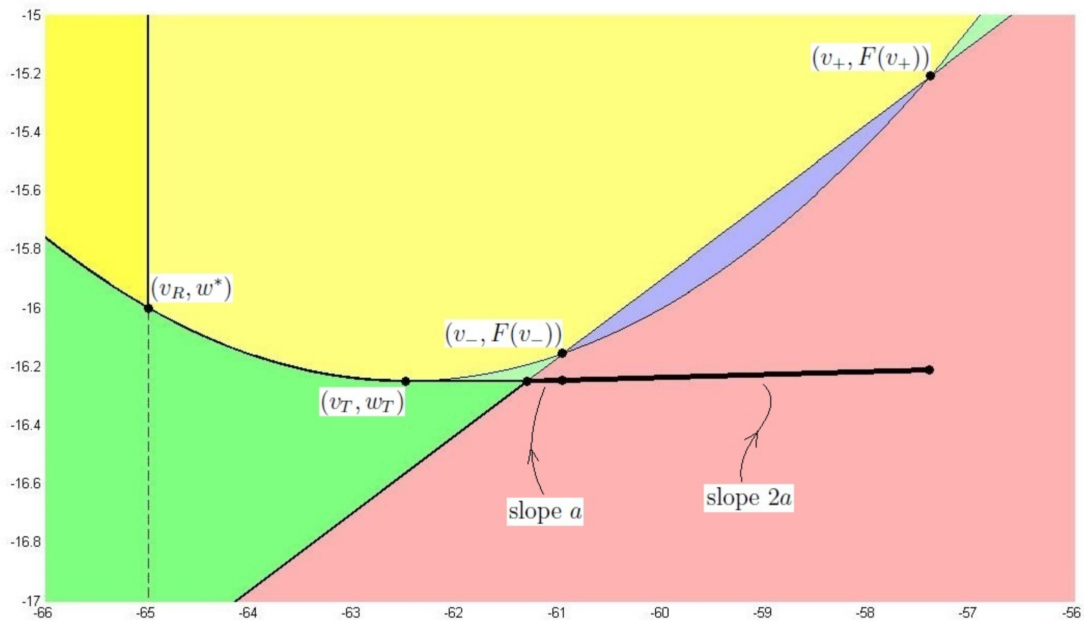

FIG. 5.6. *Upper bound curve for path segments, for $v \in [v_-, v_+]$*

$\{(v, w) : v_- < v < v_+\}$. We construct the curve depicted in Figure 5.6, and estimate the integral in (5.2) along this curve.

In Section 4 it is shown that trajectories lie in $A \cup B$ up to the w-nullcline, therefore when $v = w_T/b$ trajectories have $w < w_T$. Also, $g/f < a$ whenever the v-nullcline lies above the w-nullcline, that is, when $v \notin [v_-, v_+]$. Therefore, the line that has slope a and intersects $(w_T/b, w_T)$ lies above trajectories on the set $w_T/b \leq v \leq v_-$. Then, take another line that intersects the first line at $v = v_-$ and has slope $2a$. It can be checked that $g/f < 2a$ on this line for $v_- \leq v \leq v_+$, so that trajectories do not cross it from below. Together these lines give an upper bound curve. Discretizing the expression in (5.2) and evaluating it numerically along this upper bound curve gives the bound 1.5×10^{-3} on the integral in (5.2). □

We now estimate the negative contribution.

PROPOSITION 5.5.

$$\int_0^{r_W} J(\phi(s, x_0))dr < -1.5 \times 10^{-3} \tag{5.3}$$

Proof. The approach is to identify a region through which trajectories pass, and to estimate the integral in that region. Specifically, we carve out the channel C shown in Figure 5.7 and prove that the inequality

$$\int_{\{0 \leq r \leq r_W \,:\, \phi(r, x_0) \in C\}} J(\phi(s, x_0))ds < -1.5 \times 10^{-3}$$

holds for each trajectory. Since J is everywhere negative this implies (5.3).

In the figure there are two curves γ_α and $\gamma_{\alpha'}$ that lie parallel to the v-nullcline, and a line l_α which is the tangent line to γ_α at $v = v_R$. The channel consists of the region bounded above by $\gamma_{\alpha'}$, below by γ_α, on the left by $v_a = -64.925$ and on the right by $v_b = -63.75$. We proceed as follows.

1. For $v \leq v_b$ we show that trajectories lie above $\gamma_\alpha \cup l_\alpha$.
2. For $v_a \leq v \leq v_b$ we show that trajectories lie below $\gamma_{\alpha'}$.
3. We estimate the integral of J for trajectories in the channel.

We begin with Step 1. Take the curve γ_α that lies a distance $\alpha = 0.05$ below the v-nullcline, and take l_α, its tangent line at $v = v_R$, which has slope -0.2. On l_α, $\partial_v(g/f)$ gives a quadratic equation in v that

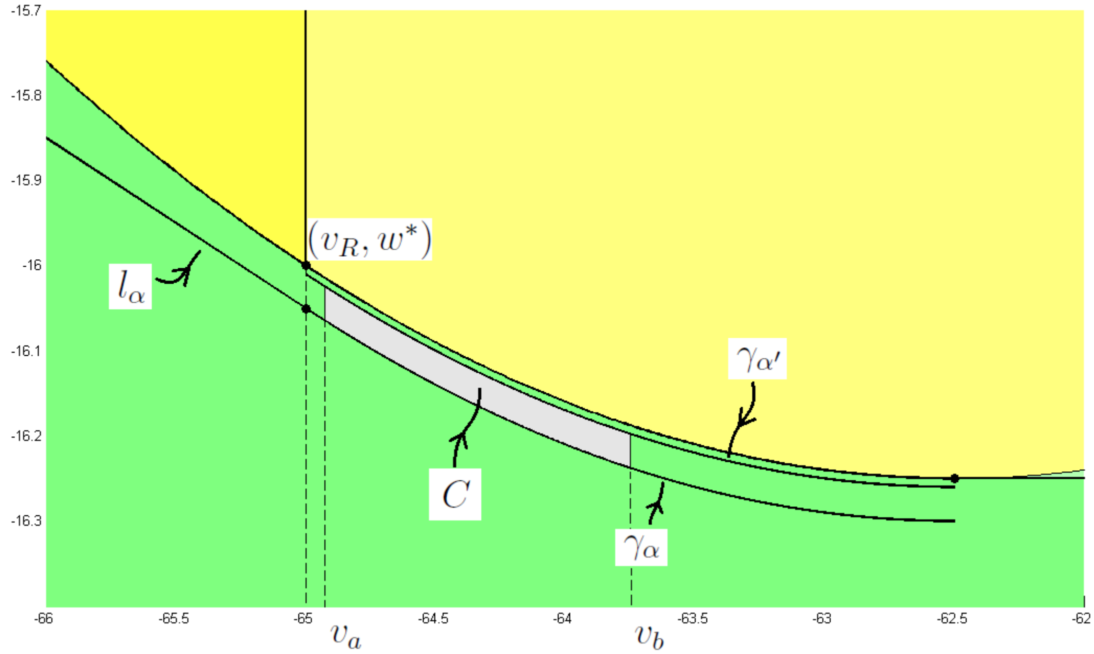

FIG. 5.7. *The channel C*

has two roots, one on either side of v_R. Also, $\partial_v(g/f) > 0$ at v_R, so that the lesser root is a minimum of g/f. The value of g/f at this root is greater than -0.2, therefore trajectories cross l_α from the left. Now, γ_α has slope F', since it lies parallel to the v-nullcline, and along γ_α, f takes the value α, and g and F' both increase with v. Therefore g has its minimum at v_R, and F' has its maximum at $v = v_b$, and it can be checked that

$$\max_{[v_R, v_b]} F'(v) = F'(v_b) < g(v_R)/\alpha = \min_{[v_R, v_b]} g/f$$

Therefore, for $v_R \leq v \leq v_b$, γ_α is crossed from below, so that together, l_α and γ_α give a lower bound on trajectories for $v \leq v_b$.

Now, we show Step 2. For $\alpha' = 0.01$ take the curve $\gamma_{\alpha'}$ that lies a distance α' below the v-nullcline. On this curve $g/f = -0.6075$ at v_R, and $g/f = -0.3369$ at v_b, and along it f is constant and $|g|$ decreases in the v direction at least up to v_b, thus $g/f \in [-0.6075, -0.3369]$ on $\gamma_{\alpha'}$, for $v \in [v_R, v_b]$. Also, $F'(v_R) = -0.2$, $F'(v_b) = -0.1$, and F' increases with v, therefore the slope of $\gamma_{\alpha'}$ takes values in $[-0.2, -0.1]$. It follows that trajectories cross $\gamma_{\alpha'}$ from above. For $v_R \leq v \leq v_b$ the trajectory with initial point (v_R, w^*) is an upper bound. Draw the line that has slope $-1/3$ and intersects (v_R, w^*). Between $\gamma_{\alpha'}$ and the v-nullcline trajectories have slope at most $-0.3369 < -1/3$ and so this line is not crossed before $\gamma_{\alpha'}$. Therefore, the intersection of the two lines gives a left-hand bound on the channel. To estimate this intersection draw the tangent line to $\gamma_{\alpha'}$ at v_R, which has slope -0.2. The two lines have initial separation $\alpha' = 0.01$ and so they intersect after a distance $0.01/(-0.2 - (-1/3)) = 0.075$. Since $v_a = -65 + 0.075 = -64.925$, then for $v_a \leq v \leq v_b$ path segments lie between γ_α and $\gamma_{\alpha'}$.

Now, we give Step 3. We want to show that

$$\int_{v_a}^{v_b} \frac{-f^2 a}{(f^2+g^2)^{3/2}} \frac{dt}{dv} dv = \int_{v_a}^{v_b} \frac{-a}{|f|(1+(g/f)^2)} dv < -1.5 \times 10^{-3} \tag{5.4}$$

along trajectories contained in C. On C, $1/|f| \geq 1/\alpha = 20$ and $|g/f| < 1$, so the integral in (5.4) is less than

$$(v_b - v_a)\frac{-a}{2\alpha} = -0.059$$

which is less than -1.5×10^{-3}. □

We have shown that the contraction integral in (3.26) is negative, from which it follows that Φ is non-expansive on (w^*, ∞). Since all orbits under Φ are eventually contained in (w^*, ∞) it follows that all orbits under Φ converge to a unique fixed point, so that all initial conditions lead to regular spiking. This concludes the proof of Theorem 5.1.

Remark 3. *For the example of the Izhikevich model, $\Phi(w^*) > w^*$ and $\Phi^2(w^*) > w^*$ as shown in Figure 5.5. From Theorem 3.3 of [16] it follows that all orbits under Φ converge either to a unique fixed point or to a periodic orbit of period 2. Therefore the result of Theorem 5.1 is a refinement of that result which is biologically relevant, since regular spiking and period 2 bursting are functionally different behaviours. Also, the above proof shows how stability can be verified by measuring the separation of orbits in the phase plane, without computing the orbits directly; in this case a Riemann sum in Proposition 5.2 is the only computer-assisted computation.*

Acknowledgements The authors thank the referees for important comments and suggestions. Lance Robson is thanked for his work on the analysis of the Izhikevich model; the example given in Section 5.3 draws from his work on the model. This research is partially supported by an IGTC fellowship to E.F., and by NSERC Discovery Grants.

REFERENCES

[1] R. Brette and W. Gerstner, *Adaptive exponential integrate-and-fire model as an effective description of neuronal activity*, J. Neurophysiol., 94 (2005), pp. 3637–3642.

[2] C. Clopath, R. Jolivet, A. Rauch, H.R. Lüscher, and W. Gerstner, *Predicting neuronal activity with simple models of the threshold type: Adaptive exponential integrate-and-fire model with two compartments*, Neurocomput., 70 (2007), pp. 1668–1673.

[3] B. Eckhardt and D. Yao, *Local lyapunov exponents in chaotic systems*, Physica D, 65 (1993), pp. 100–108.

[4] R.A. FitzHugh, *Impulses and physiological states in theoretical models of nerve membrane*, Biophys. J., 1 (1961), pp. 445–466.

[5] G. Haubs and H. Haken, *Quantities describing local properties of chaotic attractors*, Z. Phys. B, 59 (1985), pp. 459–468.

[6] R. Hermann, *Differential geometry and the calculus of variations*, Academic Press, 1968.

[7] A. L. Hodgkin and A. F. Huxley, *A quantitative description of membrane current and its application to conduction and excitation in nerve*, Journal of Physiology, 117 (1952), pp. 500–544.

[8] E. Izhikevich, *Simple model of spiking neurons*, IEEE Trans. Neural Networks, 14 (2003), pp. 1569–1572.

[9] ———, *Dynamical Systems in Neuroscience*, MIT Press, 2007.

[10] W. Lohmiller and J.-J. E. Slotine, *On contraction analysis for non-linear systems*, Automatica, 34 (1998), pp. 683–696.

[11] R.K. Miller and A.N. Michel, *Ordinary Differential Equations*, Academic Press, 1982.

[12] J. Modolo, J. Henry, and A. Beuter, *Dynamics of the subthalamo-pallidal complex in Parkinson's disease during deep brain stimulation*, J Biol Phys, 34 (2008), pp. 351–366.

[13] J.M. Nese, *Quantifying local predictability in phase space*, Physica D, 35 (1989), pp. 237–250.

[14] W. Rudin, *Principles of Mathematical Analysis*, McGraw-Hill, third ed., 1976.

[15] J. Touboul, *Bifurcation analysis of a general class of nonlinear integrate-and-fire neurons*, SIAM J. Appl. Math., 68 (2008), pp. 1045–1079.

[16] J. Touboul and R. Brette, *Spiking dynamics of bidimensional integrate-and-fire neurons*, SIAM J. Applied Dynamical Systems, 8 (2009), pp. 1462–1506.